CHAPTER
EIGHT

THERMAL ANALYSIS OF FUEL ELEMENTS

I INTRODUCTION

An accurate description of the temperature distributions in the fuel elements and the reactor structures is essential to the prediction of the lifetime behavior of these components. The temperature gradients, which control the thermal stress levels in the materials, together with the mechanical loads contribute to determination of the potential for plastic deformation at high temperatures or cracking at low temperatures. The temperature level at coolant–solid surfaces controls the chemical reactions and diffusion processes, thus profoundly affecting the corrosion process. Furthermore, the impact of the fuel and coolant temperatures on the neutron reaction rates provides an incentive for accurate modeling of the temperature behavior under transient as well as steady-state operating conditions. In this chapter the focus is on the steady-state temperature field in the fuel elements. Many of the principles applied are also useful for describing the temperature field in the structural components.

The temperature in the fuel material depends on the heat-generation rate, the fuel material properties, and the coolant and cladding temperature conditions. The rate of heat generation in a fuel pin depends on the neutron slowing rates near the fuel pin and the neutron reaction rates within the fuel, as described in Chapter 3. In return, the neutron reaction rate depends on the fuel material (both the initial composition and burnup level) and the moderator material (if present) and their temperatures. Hence an exact prediction of the fuel material temperature requires simultaneous determination of the neutronic and temperature fields, although for certain conditions it is possible to decouple the two fields. Thus it is assumed that the heat-generation rate is fixed as we proceed to obtain the fuel temperature field.

Table 8-1 Thermal properties of fuel materials

Property	U	UO_2	UC	UN
Theoretical density at room temp (kg/m^3)	19.04×10^3	10.97×10^3	13.63×10^3	14.32×10^3
Metal density* (kg/m^3)	19.04×10^3	9.67×10^3	12.97×10^3	13.60×10^3
Melting point (°C)	1133	2800	2390	2800
Stability range	Up to 665°C†	Up to m.p.	Up to m.p.	Up to m.p.
Thermal conductivity average 200–1000°C (W/m°C)	32	3.6	23 ($UC_{1.1}$)	21
Specific heat, at 100°C (J/kg °C)	116	247	146	—
Linear coefficient of expansion (/°C)		10.1×10^{-6} (400–1400°C)	11.1×10^{-6} (20–1600°C)	9.4×10^{-6} (1000°C)
Crystal structure	Below 655°C: α, orthorhombic Above 770°C: γ, body-centered cubic	Face-centered cubic	Face-centered cubic	Face-centered cubic
Tensile strength, (MPa)	344–1380‡	110	62	Not well defined

*Uranium metal density in the compound at its theoretical density.

†Addition of a small amount of Mo, Nb, Ti, or Zr extends stability up to the melting point.

‡The higher values apply to cold-worked metal.

Uranium dioxide (UO_2) has been used exclusively as fuel material in light-water power reactors ever since it was used in the Shippingport PWR in 1955. Uranium metal and its alloys have been used in research reactors. Early liquid-metal-cooled reactors relied on plutonium as a fuel and more recently on a mixture of UO_2 and PuO_2. The mid-1980s saw a resurgence in the interest in the metal as fuel in U.S.-designed fast reactors. The properties of these materials are highlighted in this chapter. UO_2 use in LWRs has been marked with satisfactory chemical and irradiation tolerance. This tolerance has overshadowed the disadvantages of low thermal conductivity and uranium atom density relative to other materials, e.g., the nitrides and carbides or even the metal itself. The carbides and nitrides, if proved not to swell excessively under irradiation, may be used in future reactors.

The general fuel assembly characteristics are given in Chapter 1. Tables 8-1 and 8-2 compare the thermal properties of the various fuel and cladding materials, respectively.

Table 8-2 Thermal properties of cladding materials

Property	Zircaloy 2	Stainless steel 316
Density (kg/m^3)	6.5×10^3	7.8×10^3
Melting point (°C)	1850	1400
Thermal conductivity (W/m°C)	13 (400°C)	23 (400°C)
Specific heat (J/kg°C)	330 (400°C)	580 (400°C)
Linear thermal expansion coefficient (/°C)	5.9×10^{-6}	18×10^{-6}

II HEAT CONDUCTION IN FUEL ELEMENTS

A General Equation of Heat Conduction

The energy transport equation (Eq. 4-123) describes the temperature distribution in a solid (which is assumed to be an incompressible material with negligible thermal expansion as far as the effects on temperature distribution are concerned). If Eq. 4-123 is written with explicit dependence on the variables $\vec{r}$ and t, it becomes:

$$\rho c_p(\vec{r},T)\frac{\partial T(\vec{r},t)}{\partial t} = \nabla \cdot k(\vec{r},T)\nabla T(\vec{r},t) + q'''(\vec{r},t) \tag{8-1}$$

Note that for incompressible materials $c_p = c_v$.

At steady state Eq. 8-1 reduces to:

$$\nabla \cdot k(\vec{r},T)\nabla T(\vec{r}) + q'''(\vec{r}) = 0 \tag{8-2}$$

Because by definition the conduction heat flux is given by $\vec{q}'' \equiv -k\nabla T$, Eq. 8-2 can be written as:

$$-\nabla \cdot \vec{q}''(\vec{r},T) + q'''(\vec{r}) = 0 \tag{8-3}$$

B Thermal Conductivity Approximations

In a medium that is isotropic with regard to heat conduction, k is a scalar quantity that depends on the material, temperature, and pressure of the medium. In a noniso-tropic medium, thermal behavior is different in different directions. Highly oriented crystalline-like materials can be significantly anisotropic. For example, thermally de-posited pyrolytic graphite can have a thermal conductivity ratio as high as 200:1 in directions parallel and normal to basal planes. For anisotropic and nonhomogeneous materials, k is a tensor, which in Cartesian coordinates can be written as:

$$\bar{\bar{k}} = \begin{pmatrix} k_{xx} & k_{xy} & k_{xz} \\ k_{yx} & k_{yy} & k_{yz} \\ k_{zx} & k_{zy} & k_{zz} \end{pmatrix} \tag{8-4}$$

For anisotropic homogeneous solids the tensor is symmetric, i.e., $k_{ij} = k_{ji}$. In most practical cases k can be taken as a scalar quantity. We restrict ourselves to this particular case of a scalar k for the remainder of this text.

As mentioned before, thermal conductivity is different for different media and generally depends on the temperature and pressure. The numerical value of k varies from practically zero for gases under extremely low pressures to about 4000 W/m°K or 7000 BTU/ft hr °F for a natural copper crystal at very low temperatures.

The change of k with pressure depends on the physical state of the medium. Whereas in gases there is a strong pressure effect on k, in solids this effect is negli-gible. Therefore the conductivity of solids is mainly a function of temperature, $k = k(T)$, and can be determined experimentally. For most metals the empirical formula [1]:

$$k = k_0[1 + \beta_0(T - T_0)] \tag{8-5}$$

gives a good fit to the data in a relatively large temperature range. The values of k_0 and β_0 are constants for the particular metal. It is evident that k_0 corresponds to the reference temperature (T_0). The value of β_0 can be positive or negative. In general, β_0 is negative for pure homogeneous metals, whereas for metallic alloys β_0 becomes positive.

In the case of nuclear fuels, the situation is more complicated because k also becomes a function of the irradiation as a result of change in the chemical and physical composition (porosity changes due to temperature and fission products).

Even when k is assumed to be a scalar, it may be difficult to solve Eq. 8-2 analytically because of its nonlinearity. The simplest way to overcome the difficulties is to transform Eq. 8-2 to a linear one, which can be done by four techniques:

1. In the case of small changes of k within a given temperature range, assume k is constant. In this case Eq. 8-2 becomes:

$$k\nabla^2 T(\vec{r}) + q'''(\vec{r}) = 0 \tag{8-6}$$

2. If the change in k over the temperature range is large, define a mean $\bar{k}$ as follows:

$$\bar{k} = \frac{1}{T_2 - T_1}\int_{T_1}^{T_2} k\, dT \tag{8-7}$$

and use Eq. 8-6 with $\bar{k}$ replacing k.

3. If an empirical formula for k exists, it may be used to obtain a single variable differential equation, which in many cases can be transformed to a relatively simple linear differential equation. For example, Eq. 8-5 can be used to write:

$$T - T_0 = \frac{k - k_0}{\beta_0 k_0} \tag{8-8}$$

so that

$$k\nabla T = \frac{k\nabla k}{\beta_0 k_0} = \frac{\nabla k^2}{2\beta_0 k_0}$$

and

$$\nabla \cdot (k\nabla T) = \frac{\nabla^2 k^2}{2\beta_0 k_0} \tag{8-9}$$

Substituting from Eq. 8-9 into Eq. 8-2, we get:

$$\nabla^2 k^2 + 2\,\beta_0 k_0 q''' = 0 \tag{8-10}$$

which is a linear differential equation in k^2.

4. Finally, the heat conduction equation can be linearized by Kirchoff's transformation, as briefly described here: In many cases it is useful to know the integral:

$$\int_{T_1}^{T_2} k(T)dT$$

where $T_2 - T_1$ is the temperature range of interest. Kirchoff's method consists of finding such integrals by solving a modified heat conduction equation. Define:

$$\theta \equiv \frac{1}{k_0} \int_{T_0}^{T} k(T)dT \tag{8-11}$$

The new variable θ can be used to give:

$$\nabla\theta = \frac{1}{k_0} \nabla \int_{T_0}^{T} k(T)dT = \frac{1}{k_0} \left[\nabla T \frac{d}{dT} \int_{T_0}^{T} k(T)dT \right] = \frac{k(T)}{k_0} \nabla T \tag{8-12}$$

From this equation we find:

$$k \nabla T = k_0 \nabla\theta \tag{8-13}$$

and

$$\nabla \cdot [k\nabla T] = k_0 \nabla^2\theta \tag{8-14}$$

Then at steady state Eq. 8-2 becomes:

$$k_0 \nabla^2\theta + q''' = 0 \tag{8-15}$$

which is a linear differential equation that can generally be solved more easily than Eq. 8-2.

In practice, the nuclear industrial computer programs have allowed common use of temperature-dependent conductivity in the numerical solutions. Eq. 8-2 can be readily solved in one-dimensional geometries, as illustrated later in this chapter. Therefore the above approaches are useful only if one is interested in analytic solutions of multidimensional problems.

III THERMAL PROPERTIES OF UO_2

The LWR fuel is composed of UO_2; hence the focus of this section is on the properties of this most widely used fuel material. In particular, the thermal conductivity, melting point, specific heat, and fractional gas release are discussed.

A Thermal Conductivity

Many factors affect the UO_2 thermal conductivity. The major factors are temperature, porosity, oxygen to metal atom ratio, PuO_2 content, pellet cracking, and burnup. A brief description of the change in k with each of these factors is discussed.

1 Temperature effects. It has been experimentally observed that $k(T)$ decreases with increasing temperature until $T = 1750°C$ and then starts to increase (Fig. 8-1). The often-used integral of $k(T)$ is also given in Figure 8-1. The polynomials representing

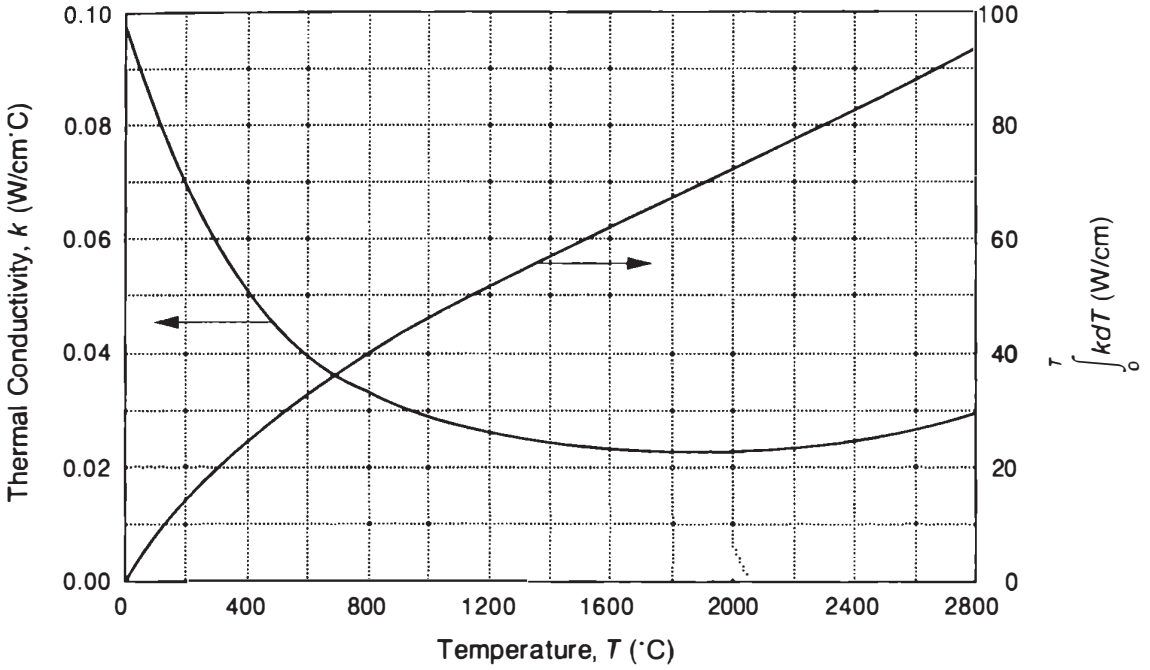

Figure 8-1 Thermal conductivity of UO_2 at 95% density from Lyon. *(From Hann et al. [9].)*

$k(T)$ proposed by the reactor vendors are given in Table 8-3. All these formulas give the value of the integral:

$$\int_{0°C}^{\text{melting}} kdT$$

as 93.5 W/cm.

For an ionic solid, thermal conductivity can be derived by assuming that the solid is an ideal gas whose particles are the quantized elastic wave vibrations in a crystal (referred to as *phonons*). It can be shown that the behavior of the UO_2 conductivity with temperature can be predicted by such a model [20].

2 Porosity (density) effects. The oxide fuel is generally fabricated by sintering pressed powdered UO_2 or mixed oxide at high temperature. By controlling the sintering conditions, material of any desired density, usually around 90% of the maximum possible or theoretical density of the solid, can be produced.

Generally, the conductivity of a solid decreases with increasing presence of voids (pores) within its structure. Hence low porosity is desirable to maximize the conductivity. However, fission gases produced during operation within the fuel result in internal pressures that may swell, and hence deform, the fuel. Thus a certain degree of porosity is desirable to accommodate the fission gases and limit the swelling potential. It is particularly true for fast reactors where the specific power level is higher, and hence the rate at which gases are produced per unit fuel volume is higher, than in thermal reactors.

Table 8-3 Formulations for UO_2 thermal conductivity at 95% theoretical density (used by reactor vendors) [25]

Temperature-dependent thermal conductivity

1. Derived from Lyon's $\int k dT$ and shown on Figure 8-1 (used by Combustion Engineering)

$$k = \frac{38.24}{402.4 + T} + 6.1256 \times 10^{-13}(T + 273)^3 \qquad \text{(Eq. 8-16a)}$$

where:
k = UO_2 conductivity (W/cm °C)
T = local UO_2 temperature (°C)

2. Composite from a variety of sources (used by Westinghouse)

$$k = \frac{1}{11.8 + 0.0238T} + 8.775 \times 10^{-13} T^3 \qquad \text{(Eq. 8-16b)}$$

where:
k = W/cm °C
T = °C

Polynomial representation of Lyon's $\int k dT$ (used by Babcock and Wilcox)

$$\begin{aligned}\int_{32}^{T} k dT = &- 170.9124 + 5.597256T - 3.368695 \times 10^{-3}T^2 \\ &+ 1.962784 \times 10^{-6}T^3 - 8.391225 \times 10^{-10}T^4 \\ &+ 2.404192 \times 10^{-13}T^5 - 4.275284 \times 10^{-17}T^6 \\ &+ 4.249043 \times 10^{-21}T^7 - 1.797017 \times 10^{-25}T^8\end{aligned} \qquad \text{(Eq. 8-16c)}$$

where:
T = °F
$\int k dT$ = Btu/hr ft

Let us define the porosity (P) as:

$$P = \frac{\text{volumes of pores } (V_p)}{\text{total volumes of pores } (V_p) \text{ and solids } (V_s)} = \frac{V_p}{V} = \frac{V - V_s}{V}$$

or

$$P = 1 - \frac{\rho}{\rho_{TD}} \qquad (8\text{-}17)$$

where ρ_{TD} is the theoretical density of the poreless solid. The effect of porosity on $\int k dT$ for mixed oxides is shown in Figure 8-2.

By considering the linear porosity to be $P^{1/3}$ and the cross-sectional porosity to be $P^{2/3}$, Kampf and Karsten [13] derived an equation for negligible pore conductance:

$$k = (1 - P^{2/3})k_{TD} \qquad (8\text{-}18)$$

Earlier, the analysis of Loeb [15] was used by Francl and Kingery [7] to derive the equation referred to as the Loeb equation for this condition of negligible pore conductance:

$$k = (1 - P)k_{TD} \qquad (8\text{-}19)$$

Equation 8-19 was found to underestimate the porosity effect.

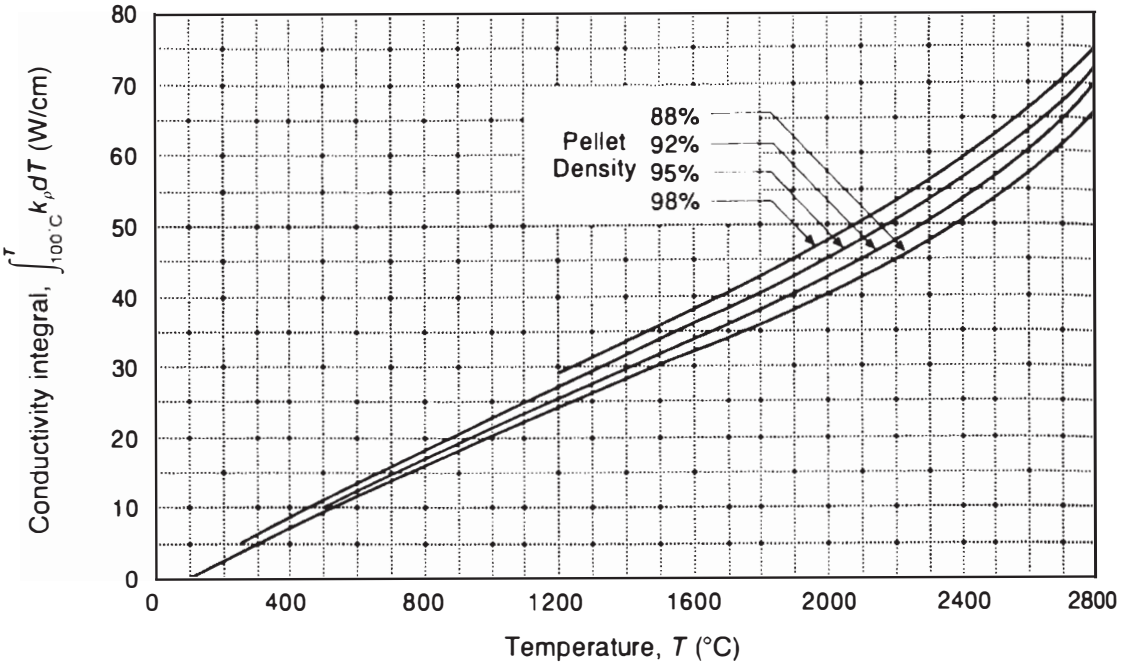

Figure 8-2 $\int_{100°C}^{T} k_p dT$ versus temperature for mixed oxide fuel. Note: 32.8 W/cm = 1 kW/ft.

A modified Loeb equation is often used to fit the UO_2 conductivity measurements as:

$$k = (1 - \alpha_1 P)k_{TD} \tag{8-20}$$

where α_1 is between 2 and 5 [20].

Biancharia [2] derived the following formula for the porosity effect, which accounts for the shape of the pores:

$$k = \frac{(1 - P)}{1 + (\alpha_2 - 1)P} k_{TD} \tag{8-21}$$

where $\alpha_2 = 1.5$ for spherical pores. For axisymmetric shapes (e.g., ellipsoids), α_2 is larger. This formula is often used in LMFBR applications.

The following fit for the temperature and porosity effects on conductivity is used in the MATPRO fuel analysis package for unirradiated fuels [22]:

For $0 \leq T \leq 1650°C$:

$$k = \eta \left[\frac{B_1}{B_2 + T} + B_3 \exp(B_4 T) \right] \tag{8-22a}$$

For $1650 \leq T \leq 2940°C$:

$$k = \eta [B_5 + B_3 \exp(B_4 T)] \tag{8-22b}$$

where k is in W/cm °C, T is in °C, and η = porosity correction factor given by:

$$\eta = \frac{1 - \beta(1 - \rho/\rho_{TD})}{1 - \beta(1 - 0.95)} \tag{8-22c}$$

Table 8-4 Values of the constants in the MATPRO correlation for thermal conductivity*

Fuel	B_1 (W/cm)	B_2 (°C)	B_3 (W/cm °C)	B_4 (°C^{-1})	B_5 (W/cm °C)
UO_2	40.4	464	1.216×10^{-4}	1.867×10^{-3}	0.0191
$(U,Pu)O_2$	33.0	375	1.540×10^{-4}	1.710×10^{-3}	0.0171

*Equations 8-22a through 8-22d.

where:

$$\beta = 2.58 - 0.58 \times 10^{-3} T \tag{8-22d}$$

and the constants B_1 through B_5 are given in Table 8-4.

3 Oxygen-to-metal atomic ratio. The oxygen-to-metal ratio of the uranium and plutonium oxides can vary from the theoretical (or stoichiometric) value of 2. This variation affects almost all the physical properties of the fuel. The departure from the initial stoichiometric condition occurs during burnup of fuel. In general, the effect of both the hyper- and hypostoichiometry is to reduce the thermal conductivity, as shown in Figure 8-3.

4 Plutonium content. Thermal conductivity of the mixed oxide fuel decreases as the plutonium oxide content increases, as can be seen in Figure 8-4.

5. Effects of pellet cracking. Fuel pellet cracking and fragment relocation into the pellet–cladding gap during operation alters the fuel thermal conductivity and the gap conductance. A series of tests at the Idaho National Engineering Laboratory have led to an empirical formula for the decrease in the UO_2 thermal conductivity due to cracking. For a fresh, helium-filled LWR fuel rod with cracked and broken fuel pellets, this relation is [16]:

$$k_e = k_{UO_2} - (0.0002189 - 0.050867 X + 5.6578 X^2) \tag{8-23a}$$

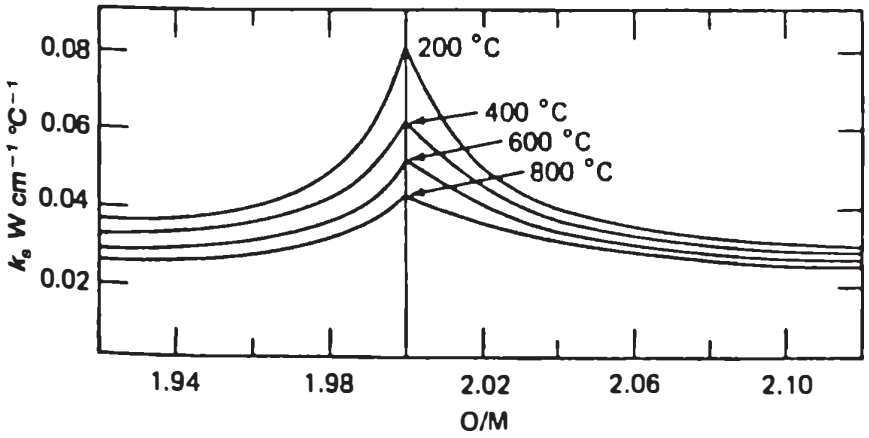

Figure 8-3 Thermal conductivity of $UO_{0.8}Pu_{0.2}O_{2\pm x}$ as a function of the O/(U + Pu) ratio. *(From Schmidt and Richter [24].)*

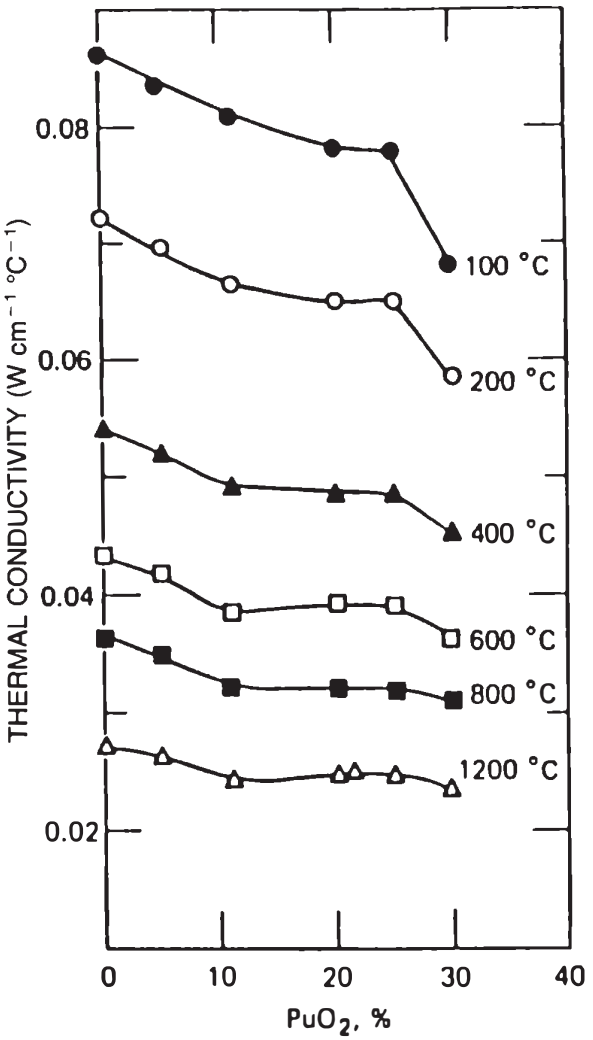

Figure 8-4 Thermal conductivity of $(U,Pu)O_2$ solid solutions as a function of PuO_2 content. *(From Gibby [8].)*

where

$$X = (\delta_{hot} - 0.014 - 0.14\ \delta_{cold}) \left(\frac{0.0545}{\delta_{cold}}\right) \left(\frac{\rho}{\rho_{TD}}\right)^8 \tag{8-23b}$$

where k is in kW/m°K; δ_{hot} = calculated hot gap width (mm) for the uncracked fuel; δ_{cold} = cold gap width (mm); ρ_{TD} = theoretical density of UO_2.

The effect of cracking on fuel conductivity is illustrated in Figure 8-5.

A semiempirical approach by MacDonald and Weisman [17] yielded the following relation between the effective conductivity and the theoretical one:

$$k_e = \frac{k_{UO_2}}{\left[\dfrac{\delta_{hot} - A}{D_{fo}(B\ k_{gas}/k_{UO_2} + C)}\right] + 1} \text{ (W/m °K)} \tag{8-24}$$

where A, B, and C = constants; D_{fo} = hot pellet diameter in meters; k_{gas} = thermal conductivity of the gas in the gap; δ_{hot} = hot gap in meters. The constants recommended are as follows:

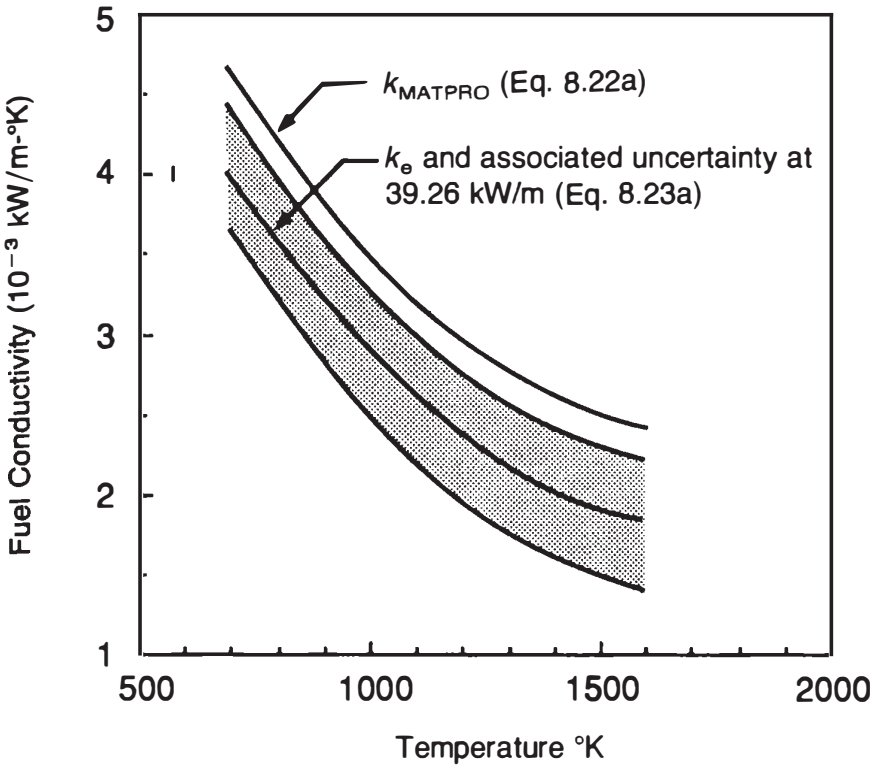

Figure 8-5 Representative comparison between MATPRO fuel thermal conductivity and calculated effective fuel thermal conductivity, with estimated uncertainty, for 2.2% initial gap helium-filled rods at a power of 39.26 kW/m. *(From MacDonald and Smith [16].)*

$A = 6.35 \times 10^{-5}$ m
$B = 0.077$
$C = 0.015$

6 Burnup The irradiation of fuel induces several changes in the porosity, composition, and stoichiometry of the fuel. These changes, however, are generally small in LWRs, where the burnup is only on the order of 3% of the initial uranium atoms. In fast reactors, this effect would be larger, as the expected burnup is on the order of 10% of the initial uranium and plutonium atoms.

Introduction of fission products into the fuel with burnup leads to a slight decrease in the conductivity. Fuel material cracking under thermal cycling also reduces the fuel effective conductivity.

Finally, the oxide material operating at temperatures higher than a certain temperature, about 1400°C, undergoes a sintering process that leads to an increase in the fuel density. This increase in density, which occurs in the central region of the fuel, affects the conductivity and the fuel temperature distribution, which is discussed in detail later.

B Fission gas release.

It is important for the design of the fuel pin to calculate the gas released to the fuel pin plenum. Some of the fission gases are released from the UO_2 pellet at low tem-

perature. Accompanying the change in the structure of the fuel at high temperatures is a significant release of fission gases to the fuel boundaries. The accumulated gases within the cladding lead to pressurization of the cladding. With engineering analysis, a simple scheme is often used in which a certain fraction (f) of the gas is assumed to be released depending on the fuel temperature. An empirically based formula is given as [19]:

$$\begin{aligned}
f &= 0.05 \qquad T < 1400°C \\
f &= 0.10 \qquad 1500 > T > 1400°C \\
f &= 0.20 \qquad 1600 > T > 1500°C \\
f &= 0.40 \qquad 1700 > T > 1600°C \\
f &= 0.60 \qquad 1800 > T > 1700°C \\
f &= 0.80 \qquad 2000 > T > 1800°C \\
f &= 0.98 \qquad T > 2000°C
\end{aligned} \tag{8-25}$$

More complicated approaches to fission gas release have been proposed based on various physical mechanisms of gas migration. Most designers, however, still prefer the simple empirically based models.

C Melting Point

The melting point of UO_2 is in the vicinity of 2840°C (5144°F). The melting process for the oxide starts at a solidus temperature but is completed at a higher temperature called the *liquidus point*. The melting range is affected by the oxygen-to-metal ratio

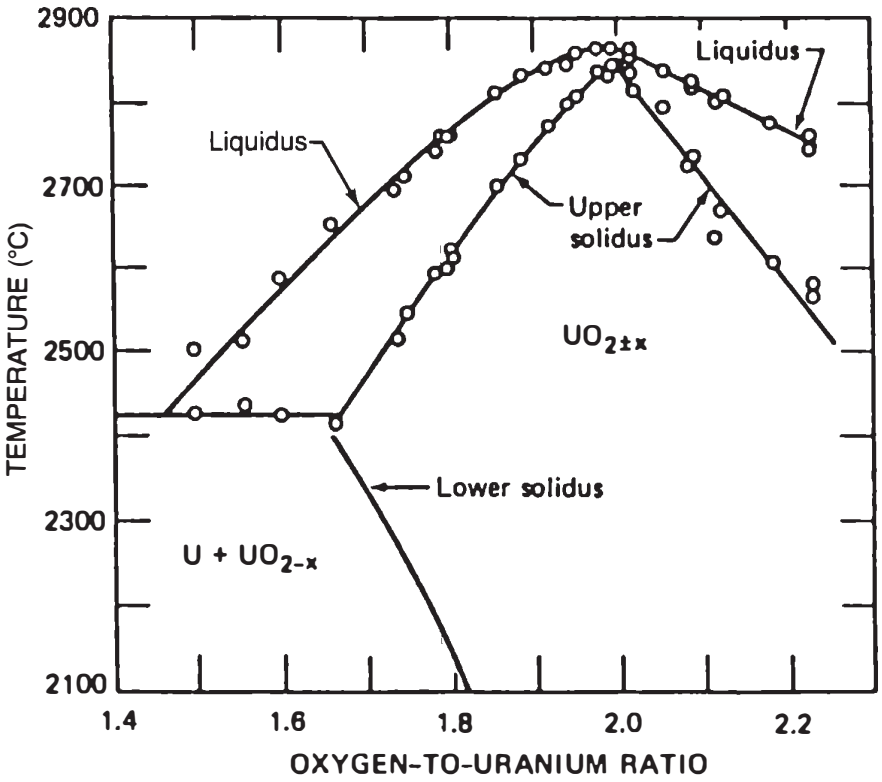

Figure 8-6 Partial phase diagram for uranium from $UO_{1.5}$ to $UO_{2.23}$ should coincide for $UO_{2.0}$. *(From Latta and Fryxell [14].)*

(Fig. 8-6) and by the Pu content. Thus in LWR designs the conservatively low value of 2600°C (4700°F) is often used. Olsen and Miller [21] fitted the melting point for MATPRO as:

$$T(\text{solidus}) = 3113 - 5.414\xi + 7.468 \times 10^{-3}\,\xi^2\ ^\circ\text{K} \qquad (8\text{-}26)$$

where ξ = mole percent of PuO_2 in the oxide. The effect of increased PuO_2 content is shown in Figure 8-7.

D Specific Heat

The specific heat of the fuel plays a significant role in determining the sequence of events in many transients. It varies greatly over the temperature range of the fuel (Fig. 8-8).

Example 8-1 Effect of cracking on fuel conductivity

PROBLEM Evaluate the effective conductivity of the fuel after cracking at 1000°C for the geometry and operating conditions given below.

1. *Geometry and materials:* BWR fuel rod with UO_2 solid fuel pellet and zircaloy clad. Cold fuel rod dimensions (at 27°C) are:
   a. Clad outside diameter = 12.52 mm
   b. Clad thickness = 0.86 mm
   c. Diametral gap width = 230 μm
2. *Assumptions*
   a. Initial fuel density = 0.88 ρ_{TD}

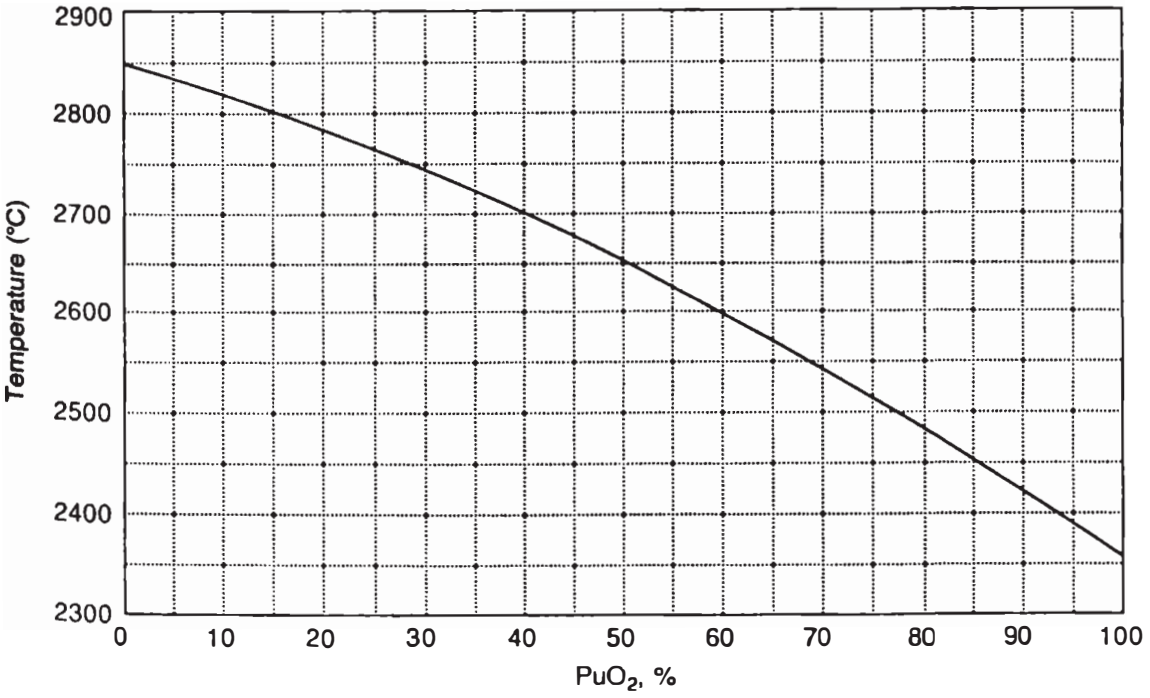

Figure 8-7 Melting points of mixed uranium–plutonium oxides. *(Adapted from Zebroski et al. [27].)*

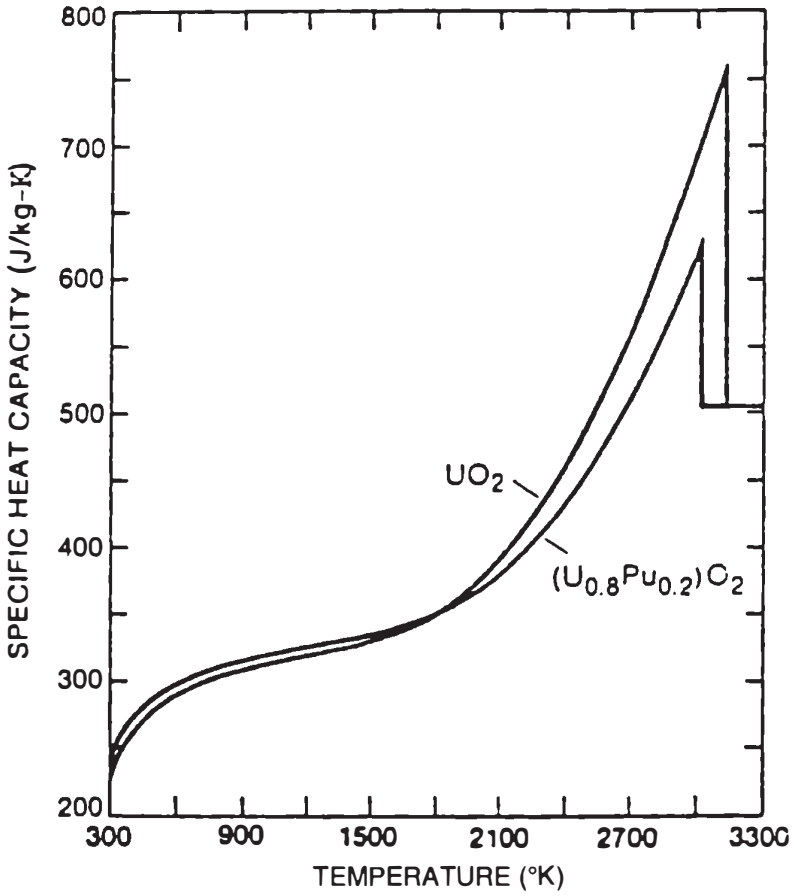

Figure 8-8 Temperature dependence of the specific heat capacity of UO_2 and $(U,Pu)O_2$ *(From Olsen and Miller [21].)*

b. UO_2 conductivity is predicted by the Westinghouse correlation in Table 8-3.
c. Porosity correction factor for the conductivity is given by Eq. 8-21 assuming spherical pores.
d. Fuel conductivity of the cracked fuel is given by Eq. 8-23a.

3. *Operating condition*
   a. Fuel temperature = 1000°C
   b. Clad temperature = 295°C

SOLUTION Consider first the conductivity of the uncracked fuel pellet. From Eq. 8-16b (Table 8-3), the UO_2 conductivity at 1000°C is:

$$\begin{aligned} k_{0.95} &= \frac{1}{11.8 + 0.0238(1000)} + 8.775 \times 10^{-13}(1000)^3 \\ &= 0.0281 + 0.00088 \\ &= 0.02898 \text{ W/cm°C} \\ &= 0.002898 \text{ kW/m°C} \end{aligned}$$

Applying the porosity correction factor of Eq. 8-21:

$$\frac{k}{k_{TD}} = \frac{1 - P}{1 + 0.5P} = \frac{\rho/\rho_{TD}}{1 + 0.5(1 - \rho/\rho_{TD})}$$

Because $\rho/\rho_{TD} = 0.88$ and 0.95 for the 88% and 95% theoretical density fuels, respectively, we get:

$$\frac{k_{0.88}}{k_{0.95}} = \frac{0.88}{1 + 0.5(0.12)} \frac{1 + 0.5(0.05)}{0.95} = (0.83)(1.079) = 0.896$$

Therefore the conductivity of the 88% theoretical density uncracked fuel pellet is:

$$k_{0.88} = 0.896\ (0.002898) = 2.597 \times 10^{-3}\ \text{kW/m°C}$$

Consider the cracked fuel effective conductivity. From Eqs. 8-23a and 8-23b:

$$k_{eff} = k_{UO_2} - (0.0002189 - 0.050867X + 5.6578X^2)\ \text{kW/m°C} \quad (8\text{-}23a)$$

$$X = (\delta_{hot} - 0.014 - 0.14\delta_{cold}) \left(\frac{0.0545}{\delta_{cold}}\right) \left(\frac{\rho}{\rho_{TD}}\right)^8 \quad (8\text{-}23b)$$

For the cold gap, $\delta_{cold} = 0.23$ mm as given. To evaluate δ_{hot}, we must evaluate the change in the radius of the fuel and the cladding. If the fuel pellet radius is R_{fo} and the cladding inner radius is R_{ci}:

$$\begin{aligned}\delta_{hot} &= (R_{ci})_{hot} - (R_{fo})_{hot} \\ &= (R_{ci})_{cold}[1 + \alpha_c(T_c - 27)] - (R_{fo})_{cold}[1 + \alpha_f(T_f - 27)]\end{aligned}$$

where α = linear thermal expansion coefficient.
However,

$$(R_{ci})_{cold} = \frac{12.52}{2} - 0.86 = 5.40\ \text{mm}$$

and

$$(R_{fo})_{cold} = \frac{12.52}{2} - 0.86 - 0.23 = 5.17\ \text{mm}$$

From Table 8-1, $\alpha_f = 10.1 \times 10^{-6}$ per°C
From Table 8-2, $\alpha_c = 5.9 \times 10^{-6}$ per°C
Therefore $\delta_{hot} = 5.40[1 + 5.9 \times 10^{-6}(295 - 27)] - 5.17[1 + 10.1 \times 10^{-6}(1000 - 27)] = 5.40854 - 5.22081 = 0.18773$ mm

Now we can determine the parameter X from Eq. 8-23b:

$$\begin{aligned}X &= [0.18773 - 0.014 - 0.14(0.23)] \left[\frac{0.0545}{0.23}\right] [0.88]^8 \\ &= 0.14153(0.23696)(0.35963) \\ &= 0.01206\end{aligned}$$

Hence the cracked fuel conductivity for the 88% theoretical density fuel is given by Eq. 8-23a as:

$$\begin{aligned}k_{eff} &= 0.896(0.002898) - [0.0002189 - 0.050867(0.01206) + 5.6578(0.01206)^2] \\ &= 0.0026 - (0.0002189 - 0.000613 + 0.000823) \\ &= 0.0026 - (0.000439) \\ &= 0.002161\ \text{kW/m °C}\end{aligned}$$

Thus the effect of cracking is to reduce the fuel effective thermal conductivity in this fuel from 2.60 to 2.16 W/m °C.

IV TEMPERATURE DISTRIBUTION IN PLATE FUEL ELEMENTS

A General Conduction Equation in Cartesian Coordinates

Assume a fuel plate is operating with a uniform heat-generation rate (q'''). The fuel is clad in thin metallic sheets, with perfect contact between the fuel and the cladding as shown in Figure 8-9.

If the fuel plate is thin and extends in the y and z directions considerably more than it does in the x direction, the heat conduction equation (Eq. 8-2):

$$\frac{\partial}{\partial x} k \frac{\partial T}{\partial x} + \frac{\partial}{\partial y} k \frac{\partial T}{\partial y} + \frac{\partial}{\partial z} k \frac{\partial T}{\partial z} + q''' = 0 \tag{8-27}$$

can be simplified by assuming the heat conduction in the y and z directions to be negligible, i.e.,

$$k \frac{\partial T}{\partial y} \simeq k \frac{\partial T}{\partial z} \simeq 0 \tag{8-28}$$

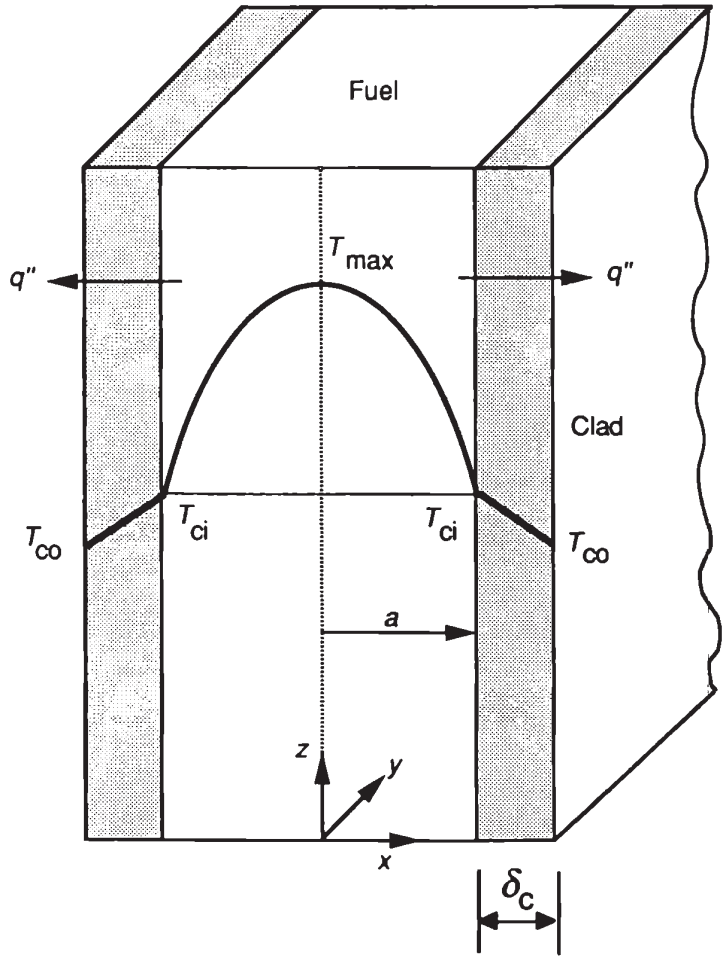

Figure 8-9 Plate fuel element.

Hence, we need only to solve the one-dimensional equation:

$$\frac{d}{dx} k \frac{dT}{dx} + q''' = 0 \tag{8-29}$$

By integrating once, we get:

$$k \frac{dT}{dx} + q''' x = C_1 \tag{8-30}$$

B Application to a Fuel Plate

Because q''' is uniform, and if the temperatures at both interfaces between cladding and fuel are equal, the fuel temperature should be symmetric around the center plane. In the absence of any heat source or sink at $x = 0$, no heat flux should cross the plane at $x = 0$. Hence:

$$k \frac{dT}{dx}\bigg|_{x=0} = 0 \tag{8-31}$$

Applying the condition of Eq. 8-31 to Eq. 8-30 leads to:

$$C_1 = 0 \tag{8-32}$$

and

$$k \frac{dT}{dx} + q'''x = 0 \tag{8-33}$$

Integrating Eq. 8-33 between $x = 0$ and any position x, and applying the condition that $T = T_{max}$ at $x = 0$, we get:

$$\int_{T_{max}}^{T} k dT + q''' \frac{x^2}{2}\bigg|_0^x = 0$$

or

$$\int_{T}^{T_{max}} k\, dT = q''' \frac{x^2}{2} \tag{8-34}$$

Three conditions may exist, depending on whether q''', T_{ci}, or T_{max} are known.

1. q''' specified: A relation between T_{max} and T_{ci} can be determined when q''' is specified by substituting $x = a$ in Eq. 8-34 to get:

$$\int_{T_{ci}}^{T_{max}} k dt = q''' \frac{a^2}{2} \tag{8-35}$$

If k = constant,

$$k(T_{max} - T_{ci}) = q''' \frac{a^2}{2} \tag{8-36}$$

2. T_{ci} specified: If T_{ci} is known, Eq. 8-34 can be used to specify the relation between q''' and T_{max} in the form:

$$q''' = \frac{2}{a^2} \int_{T_{ci}}^{T_{max}} k dT \tag{8-37}$$

3. T_{max} specified: Equation 8-37 can be used to specify the relation between q''' and T_{ci} given the value of T_{max}.

C Heat Conduction in Cladding

The heat conduction in the cladding can also be assumed to be a one-dimensional problem, so that Eq. 8-29 also applies in the cladding. Furthermore, the heat generation in the cladding is negligible (mainly owing to absorption of γ rays and inelastic scattering of neutrons). Hence in the cladding the heat conduction equation is given by:

$$\frac{d}{dx} k_c \frac{dT}{dx} = 0 \tag{8-38}$$

Integrated once, it leads to the equation:

$$k_c \frac{dT}{dx} = B_1 = \text{constant} \tag{8-39}$$

which implies that the heat flux is the same at any position in the cladding. Let q'' be the heat flux in the cladding in the outward x direction. Therefore:

$$- k_c \frac{dT}{dx} = q'' \tag{8-40}$$

Integrating Eq. 8-40 between $x = a$ and any position x leads to:

$$\int_{T_{ci}}^{T} k_c dT = - q''(x - a) \tag{8-41}$$

or

$$\bar{k}_c(T - T_{ci}) = - q''(x - a) \tag{8-42}$$

where $\bar{k}_c$ = average clad conductivity in the temperature range.

Thus the external clad surface temperature is given by:

$$\bar{k}_c(T_{co} - T_{ci}) = -q''(a + \delta_c - a) \tag{8-43}$$

or

$$T_{co} = T_{ci} - \frac{q''\delta_c}{\bar{k}_c} \tag{8-44}$$

where δ_c = cladding thickness.

D Thermal Resistances

Note that q'' is equal to the heat generated in one-half of the fuel plate. Thus:

$$q'' = q''' a \tag{8-45}$$

Therefore the fuel temperature drop may also be obtained by substituting for $q'''a$ from Eq. 8-45 into Eq. 8-36 and rearranging the result:

$$T_{ci} = T_{max} - q'' \frac{a}{2k} \tag{8-46}$$

Substituting for T_{ci} from Eq. 8-46 into Eq. 8-44, we get:

$$T_{co} = T_{max} - q'' \left(\frac{a}{2k} + \frac{\delta_c}{k_c} \right) \tag{8-47}$$

By simple manipulation of Eq. 8-47, the heat flux q'' can be given as:

$$q'' = \frac{T_{max} - T_{co}}{\frac{a}{2k} + \frac{\delta_c}{k_c}} \tag{8-48}$$

Thus the temperature difference acts analogously to an electrical potential difference that gives rise to a current (q'') whose value is dependent on two thermal resistances in series (Fig. 8-10). This concept of resistances proves useful for simple transient fuel temperature calculations.

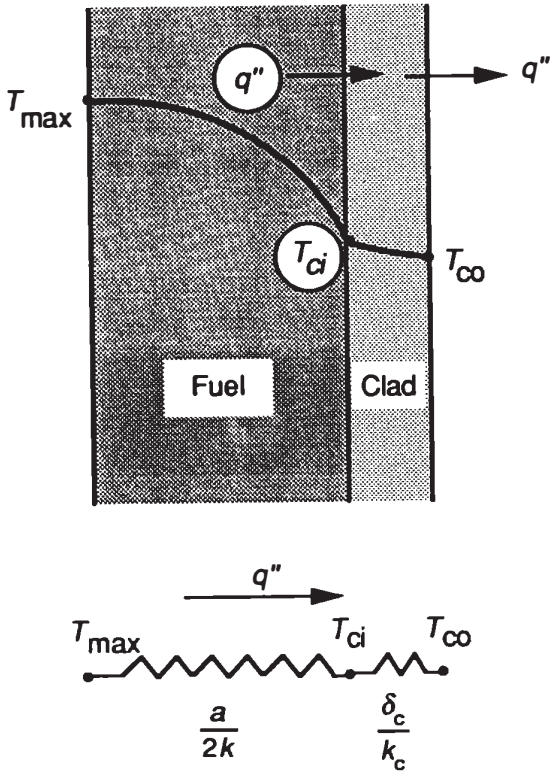

Figure 8-10 Electrical current equivalence with the heat flux.

E Conditions for Symmetric Temperature Distributions

The temperature field symmetry in the preceding discussion enabled us to solve for the temperature by considering only one-half the plate. It is useful to reflect on the required conditions to produce such symmetry.

Consider the general case for a plate fuel element with internal heat generation that is cooled on both sides (Fig. 8-11). In this case some of the heat is removed from the right-hand side, and the rest is removed from the left-hand side. Therefore a plane exists within the fuel plate through which no heat flux passes. Let the position of this plane be x_0. Thus:

$$q''|_{x_0} = k \left.\frac{\partial T}{\partial x}\right|_{x_0} = 0 \tag{8-49}$$

The value of x_0 is zero if symmetry of the temperature distribution exists. This symmetry can be a priori known under specific conditions, all of which should be present simultaneously. These conditions are the following:

1. Symmetric distribution of heat generation in the fuel plate
2. Equal resistances to heat transfer on both sides of the plate, which translates into similar material and geometric configurations on both sides (i.e., uniform fuel, fuel–clad gap, and clad material thicknesses)
3. Equal temperatures of the outermost boundary of the plate on both sides, i.e., $T_{co|A} = T_{co|B}$

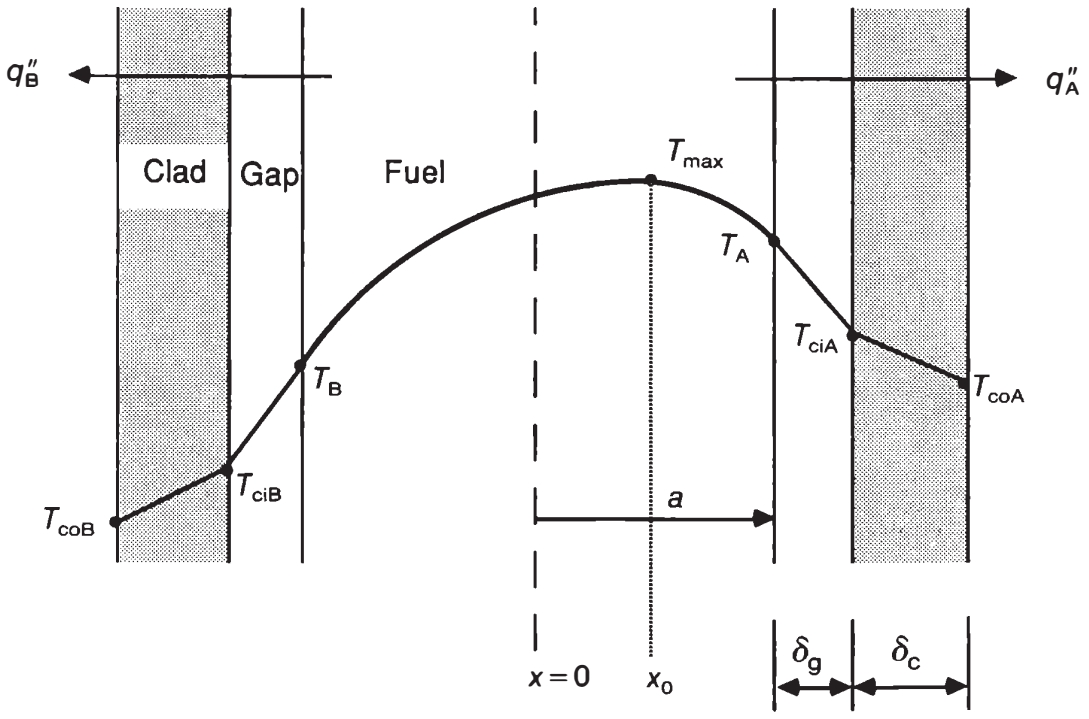

Figure 8-11 Plate with asymmetric temperature distribution.

If the three conditions exist in a fuel element, symmetry of the temperature field can be ascertained and the condition of zero heat flux at the midplane can be supplied, i.e., $x_0 = 0$ in Eq. 8-49:

$$k \left.\frac{\partial T}{\partial x}\right|_0 = 0 \tag{8-50}$$

Two examples can be cited as violating the conditions of symmetry mentioned above.

1. Nonuniform heat generation due to absorption of an incident flux of γ rays, as occurs in a core barrel or thermal shield (see Chapter 3, Section VII)
2. Nonidentical geometry of the region surrounding the fuel as happens in an off-center fuel element

In a general coordinate system the condition of symmetry is as follows.

$$\begin{aligned} \nabla T = 0 \text{ at } x &= 0 \text{ (plate)} \\ \text{at } r &= 0 \text{ (cylinder)} \\ \text{at } r &= 0 \text{ (sphere)} \end{aligned} \tag{8-51}$$

For condition 8-51 to be valid, it is implied that the fuel elements are solid. If there is a central void, condition 8-51 is not useful for solution of the temperature profile within the fuel region. When an inner void exists, and if a symmetric condition of temperature field applies, no heat flux would exist at the void boundary. This situation is illustrated for cylindrical pins in the following section.

V TEMPERATURE DISTRIBUTION IN CYLINDRICAL FUEL PINS

We derive first the basic relations for cylindrical (solid and annular) fuel pellets. Then some conclusions are made with regard to: (1) the maximum fuel temperature (T_{max}) for a given linear heat rate (q'); and (2) the maximum possible heat rate (q'_{max}) for a given T_{max}.

Cylindrical fuel pellets are nearly universally used as the fuel form in power reactors. Dimensions of the fuel pellet and cladding are given in Table 1-3.

A General Conduction Equation for Cylindrical Geometry

If the neutron flux is assumed to be uniform within the fuel pellet, the heat-generation rate can be assumed uniform. The coolant turbulent flow conditions in a fuel assembly of a pin pitch-to-diameter ratio of more than 1.2 is such that the azimuthal flow conditions can be taken to be essentially the same around the fuel rod. (More information on the azimuthal heat flux distribution is available in Chapter 7, Vol. II.) The above two conditions lead to the conclusion that no significant azimuthal temperature gradients exist in the fuel pellet. Also, for a fuel pin of a length-to-diameter ratio of

more than 10, it is safe to neglect the axial heat transfer within the fuel relative to the radial heat transfer for most of the pin length. However, near the top and bottom ends, axial heat conduction plays a role in determining the temperature field.

Thus at steady state the heat conduction equation reduces to a one-dimensional equation in the radial direction:

$$\frac{1}{r}\frac{d}{dr}\left(kr\frac{dT}{dr}\right) + q''' = 0 \tag{8-52}$$

Integrating Eq. 8-52 once, we get:

$$kr\frac{dT}{dr} + q'''\frac{r^2}{2} + C_1 = 0 \tag{8-53}$$

which can be written as:

$$k\frac{dT}{dr} + q'''\frac{r}{2} + \frac{C_1}{r} = 0 \tag{8-54}$$

For an annular fuel pellet with an internal cavity radius (R_v) (Fig. 8-12), no heat flux exists at R_v. For a solid pellet, $R_v = 0$, no heat flux exists at $r = 0$. Hence the general heat flux condition that can be applied is:

$$q''|_{r=R_v} = -k\left.\frac{dT}{dr}\right|_{r=R_v} = 0 \tag{8-55}$$

Applying this condition to Eq. 8-54 leads to:

$$C_1 = -\frac{q''' R_v^2}{2} \tag{8-56}$$

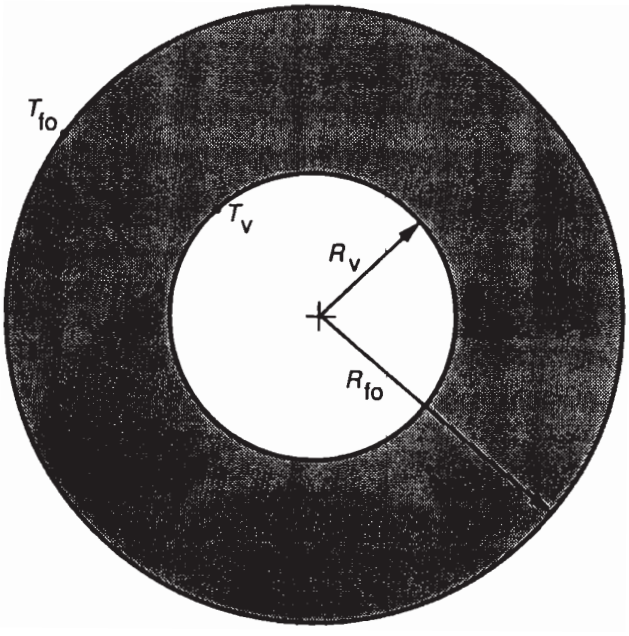

Figure 8-12 Cross section of an annular pellet.

Equation 8-54 can be integrated between r and R_v and r to yield, after rearrangement:

$$-\int_{T_{max}}^{T} k dT = \frac{q'''}{4}[r^2 - R_v^2] + C_1 \ell n \left(\frac{r}{R_v}\right) \tag{8-57}$$

B Solid Fuel Pellet

For a solid fuel pellet, applying Eq. 8-56:

$$R_v = 0 \quad \text{and} \quad C_1 = 0 \tag{8-58}$$

Hence, Eq. 8-57 becomes:

$$\int_{T}^{T_{max}} k dT = \frac{q''' r^2}{4} \tag{8-59}$$

A relation between T_{max}, T_{fo}, and R_{fo} can be obtained by Eq. 8-59 at $r = R_{fo}$ to get:

$$\int_{T_{fo}}^{T_{max}} k dT = \frac{q''' R_{fo}^2}{4} \tag{8-60}$$

The linear heat rate is given by:

$$q' = \pi R_{fo}^2 q''' \tag{8-61}$$

Therefore:

$$\int_{T_{fo}}^{T_{max}} k dT = \frac{q'}{4\pi} \tag{8-62}$$

It is interesting to note that the temperature difference across a solid fuel pellet is fixed by q' and is independent of the pellet radius (R_{fo}). Thus a limit on q' is directly implied by a design requirement on the maximum fuel temperature.

It should also be mentioned, and the student can verify on his or her own, that for a constant conductivity the average temperature in a fuel pin is given by:

$$T_{ave} - T_{fo} = \frac{1}{2}(T_{max} - T_{fo}) = \frac{q'}{8\pi k}$$

C Annular Fuel Pellet

For an annular pellet, C_1 from Eq. 8-56 can be substituted for in Eq. 8-57 to get:

$$-\int_{T_{max}}^{T} k dT = \frac{q'''}{4}[r^2 - R_v^2] - \frac{q''' R_v^2}{2} \ell n (r/R_v)$$

The above equation can be rearranged into:

$$\int_{T}^{T_{max}} k dT = \frac{q''' r^2}{4}\left\{\left[1 - \left(\frac{R_v}{r}\right)^2\right] - \left(\frac{R_v}{r}\right)^2 \ell n \left(\frac{r}{R_v}\right)^2\right\} \tag{8-63}$$

Equation 8-63 can be used to provide a relation between T_{max}, T_{fo}, R_v, and R_{fo}, when the condition $T = T_{fo}$ at $r = R_{fo}$ is applied. Thus we get:

$$\int_{T_{fo}}^{T_{max}} k dT = \frac{q''' R_{fo}^2}{4} \left\{ \left[1 - \left(\frac{R_v}{R_{fo}} \right)^2 \right] - \left(\frac{R_v}{R_{fo}} \right)^2 \ell n \left(\frac{R_{fo}}{R_v} \right)^2 \right\} \tag{8-64}$$

Note that the linear heat rate is given by:

$$q' = \pi (R_{fo}^2 - R_v^2) q''' \tag{8-65}$$

so that:

$$q''' R_{fo}^2 = \frac{q'}{\pi \left[1 - \left(\frac{R_v}{R_{fo}} \right)^2 \right]} \tag{8-66}$$

Substituting for $q''' R_{fo}^2$ from Eq. 8-66 into Eq. 8-64, we get:

$$\int_{T_{fo}}^{T_{max}} k dT = \frac{q'}{4\pi} \left[1 - \frac{\ell n (R_{fo}/R_v)^2}{\left(\frac{R_{fo}}{R_v} \right)^2 - 1} \right] \tag{8-67}$$

If a void factor is defined as:

$$F_v(\alpha, \beta) \equiv 1 - \frac{\ell n(\alpha^2)}{\beta^2(\alpha^2 - 1)} \tag{8-68}$$

Equation 8-67 can be written as:

$$\int_{T_{fo}}^{T_{max}} k dT = \frac{q'}{4\pi} \left[F_v \left(\frac{R_{fo}}{R_v}, 1 \right) \right] \tag{8-69}$$

The value of $\beta = 1$ is encountered in fuel elements of uniform power density. For nonuniform power density $\beta \neq 1$. If the power density for an inner region is higher than that of the outer region, $\beta > 1$. This situation is encountered in restructured fuel pellet analysis (section VI).

Figure 8-13 provides a plot of F_v in terms of α and β. Note that F_v is always less than 1. Hence when comparing the solid and annular pellets, the following conclusions can be made by observing Eqs. 8-62 and 8-67.

1. For the same temperature limit T_{max}:

$$q'_{annular} F_v = q'_{solid} \tag{8-70}$$

provided that T_{fo} and k are the same in the annular element as in the solid. Hence:

$$q'_{annular} > q'_{solid} \tag{8-71}$$

That is, an annular pellet can operate at a higher linear heat rate than a solid pellet if T_{max}, T_{fo}, and k are the same.

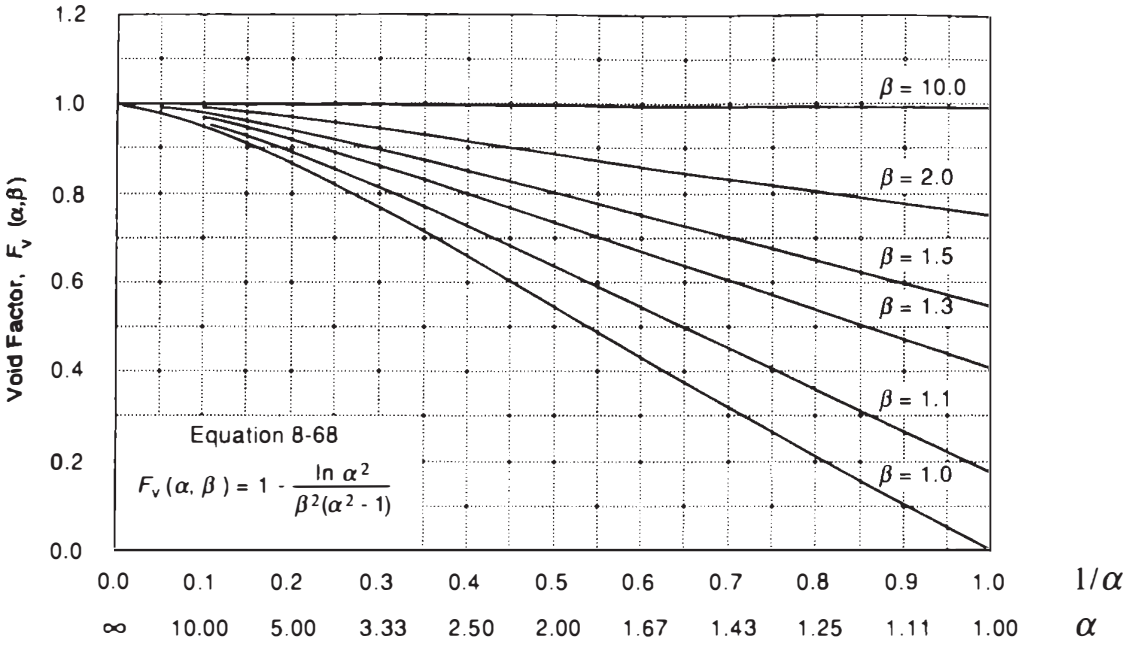

Figure 8-13 Void factor function. Note that for an annular region α is the ratio of the outer to the inner radius, and β is a function of the radii as well as the heat-generation profile in the pellet.

2. For the same heat rate (q') the temperature integrals of the conductivity are related by:

$$\left(\int_{T_{fo}}^{T_{max}} k_{annular}\, dT\right) = \left(\int_{T_{fo}}^{T_{max}} k_{solid}\, dT\right) F_v \tag{8-72}$$

so that if the fuel material conditions are the same, i.e., the same $k(T)$, and T_{fo} is the same, we get:

$$T_{max}|_{annular} < T_{max}|_{solid} \tag{8-73}$$

In this case the maximum operating temperature of the annular fuel is less than that of the solid fuel pellet.

Note that the conductivity integral is a function of the fuel pellet density, which depends on the initial fuel manufacturing conditions and irradiation conditions in the reactor. This dependence was discussed in section III. The conditions of Eqs. 8-71 and 8-73 do not necessarily apply if $k(T)$ of the annular fuel does not equal $k(T)$ of the solid fuel.

Example 8-2 Linear power of a cylindrical fuel pellet

PROBLEM For the geometry of the BWR pellet described in Example 8-1, evaluate the linear power of the pin when the fuel outer temperature is 495°C and the centerline fuel temperature is 1400°C. Assume that the fuel density is 88% ρ_{TD}, and ignore the effect of cracking on fuel conductivity.

SOLUTION

The linear power is related to the temperature difference by Eq. 8-62:

$$\int_{T_{fo}}^{T_{max}} k dT = \frac{q'}{4\pi} \tag{8-62}$$

which can be used to write:

$$q' = 4\pi \left(\int_{100}^{T_{max}} k dT - \int_{100}^{T_{fo}} k dT \right)$$

Applying the conditions specified in the problem, we get:

$$\begin{aligned} q' &= 4\pi \left(\int_{100}^{1400°C} k_{0.88}\, dT - \int_{100}^{495} k_{0.88}\, dT \right) \\ &= 4\pi(27.5 - 8.5) \text{ W/cm} \\ &= 239 \text{ W/cm} \\ &= 23.9 \text{ kW/m} \end{aligned}$$

VI TEMPERATURE DISTRIBUTION IN RESTRUCTURED FUEL ELEMENTS

Operation of an oxide fuel material at a high temperature leads to alterations of its morphology. The fuel region in which the temperature exceeds a certain sintering temperature experiences loss of porosity. In a cylindrical fuel pellet the inner region is restructured to form a void at the center, surrounded by a dense fuel region. In fast reactors, where the fuel may have a higher temperature near the center, restructuring was found to lead to three distinct regions (Fig. 8-14). In the outermost ring, where no sintering (i.e., no densification) occurs, the fuel density remains equal to the original (as fabricated) density, whereas the intermediate and inner regions have densities of 95 to 97% and 98 to 99%, respectively. It should be noted that most of the restructuring occurs within the first few days of operation, with slow changes afterward. In LWRs, where the fuel temperature is not as high as in liquid-metal-cooled reactors, two-region pellet restructuring may occur in the core regions operating at high powers. The sintering temperatures as well as the density in each fuel structure are not universally agreed on, as seen in Table 8-5.

Table 8-5 Fuel sintering temperature and densities

	Columnar grains		Equiaxed grains	
Recommendation source	T_1 (°C)	ρ_1/ρ_{TD}	T_2 (°C)	ρ_2/ρ_{TD}
Atomics International	1800	0.98	1600	0.95
General Electric	2150	0.99	1650	0.97
Westinghouse	2000	0.99	1600	0.97

Source: From Marr and Thompson [18].

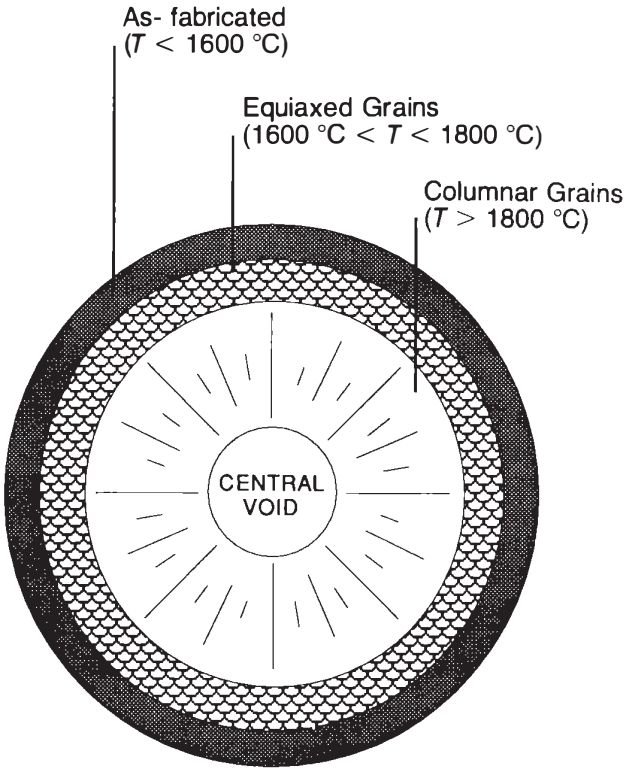

Figure 8-14 Restructuring of an oxide fuel pellet during high-temperature irradiation.

In this section, the heat conduction problem in cylindrical fuel elements that have undergone some irradiation, and hence developed sintered (densified) regions, is solved. Temperature distributions are obtained on the assumption that the fuel element may be represented by three zones (Fig. 8-15). The two-zone fuel temperature distribution is obtained by inference from the three-zone treatment.

A Mass Balance

From conservation of mass across a section in the fuel rod before and after restructuring, we conclude that the original mass is equal to the sum of the fuel mass in the three rings. Hence when the pellet length is assumed unchanged:

$$\pi R_{\text{fo}}^2 \rho_0 = \pi(R_1^2 - R_{\text{v}}^2)\rho_1 + \pi(R_2^2 - R_1^2)\rho_2 + \pi(R_{\text{fo}}^2 - R_2^2)\rho_3 \qquad (8\text{-}74)$$

However, the initial density ρ_0 is equal to ρ_3, so that an explicit expression for R_{v} can be obtained from Eq. 8-74 as:

$$R_{\text{v}}^2 = \left(\frac{\rho_1 - \rho_2}{\rho_1}\right) R_1^2 + \left(\frac{\rho_2 - \rho_3}{\rho_1}\right) R_2^2 \qquad (8\text{-}75)$$

B Power Density Relations

For a uniform neutron flux the heat-generation density is proportional to the mass density:

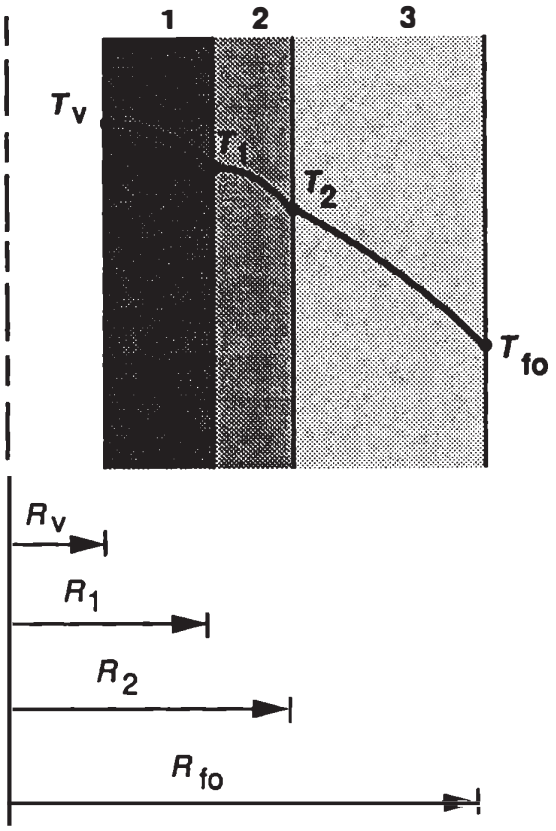

Figure 8-15 Temperature profile in a three-zone restructured fuel pellet.

$$q'''_2 = \frac{\rho_2}{\rho_3} q'''_3 \tag{8-76}$$

and

$$q'''_1 = \frac{\rho_1}{\rho_3} q'''_3 \tag{8-77}$$

However, the linear heat rate is given by the summation of the heat-generation rate in the three rings. Therefore the linear heat-generation rate in the restructured fuel (q'_{res}) is given by:

$$q'_{res} = q'''_3 \pi(R_{fo}^2 - R_2^2) + q'''_2 \pi(R_2^2 - R_1^2) + q'''_1 \pi(R_1^2 - R_v^2) \tag{8-78}$$

or

$$q'_{res} = q'''_3 \left[\pi(R_{fo}^2 - R_2^2) + \frac{\rho_2}{\rho_3} \pi(R_2^2 - R_1^2) + \frac{\rho_1}{\rho_3} \pi(R_1^2 - R_v^2) \right] \tag{8-79}$$

Combining Eqs. 8-74 and 8-79, we obtain:

$$q'_{res} = \pi R_{fo}^2 q'''_3 \tag{8-80}$$

i.e.,

$$q'''_3 = \frac{q'_{res}}{\pi R_{fo}^2} \tag{8-81}$$

That is, the power density in the as-fabricated region can be obtained from the assumption that the mass is uniformly distributed in the fuel pellet. It is equivalent to expecting the power density in the outer region not to be affected by the redistribution of the fuel within the other two zones.

C Heat Conduction in Zone 3

The differential equation is:

$$\frac{1}{r}\frac{d}{dr}\left(rk_3\frac{dT}{dr}\right) = -q'''_3 \tag{8-82}$$

By integrating once we get:

$$k_3\frac{dT}{dr} = -q'''_3\frac{r}{2} + \frac{C_3}{r} \tag{8-83}$$

and integrating again between the zone boundaries:

$$\int_{T_2}^{T_{fo}} k_3 dT = -q'''_3\frac{R_{fo}^2 - R_2^2}{4} + C_3\,\ell n\left(\frac{R_{fo}}{R_2}\right) \tag{8-84}$$

Using Eq. 8-81 we can evaluate the temperature gradient at R_{fo} from the heat flux as follows:

$$q''_{R_{fo}} = -k_3\left.\frac{dT}{dr}\right|_{R_{fo}} = \frac{q'_{res}}{2\pi R_{fo}} = q'''_3\frac{\pi R_{fo}^2}{2\pi R_{fo}} = \frac{q'''_3 R_{fo}}{2} \tag{8-85}$$

Equation 8-85 provides a boundary condition to be satisfied by Eq. 8-83. This condition leads to:

$$C_3 = 0 \tag{8-86}$$

Hence Eq. 8-84 reduces to:

$$\int_{T_{fo}}^{T_2} k_3 dT = \frac{q'''_3}{4}R_{fo}^2\left[1 - \left(\frac{R_2}{R_{fo}}\right)^2\right] \tag{8-87}$$

which, using Eq. 8-81, can also be written as:

$$\int_{T_{fo}}^{T_2} k_3 dT = \frac{q'_{res}}{4\pi}\left[1 - \left(\frac{R_2}{R_{fo}}\right)^2\right] \tag{8-88}$$

D Heat Conduction in Zone 2

The heat conduction equation integration for zone 2 leads to an equation similar to Eq. 8-83 but applicable to zone 2:

$$k_2\frac{dT}{dr} = -q'''_2\frac{r}{2} + \frac{C_2}{r} \tag{8-89}$$

At R_2, continuity of heat flux leads to:

$$\underbrace{-k_2 \left.\frac{dT}{dr}\right|_{R_2}}_{\text{From zone 2}} \text{ From zone 2} = \underbrace{-k_3 \left.\frac{dT}{dr}\right|_{R_2}}_{\text{From zone 3}} \text{ From zone 3} \tag{8-90}$$

Substituting from Eqs. 8-83 (with $C_3 = 0$) and 8-89 into Eq. 8-90 leads to:

$$+ q_2''' \frac{R_2}{2} - \frac{C_2}{R_2} = q_3''' \frac{R_2}{2}$$

or

$$C_2 = \frac{R_2^2}{2} [q_2''' - q_3'''] \tag{8-91}$$

By integrating Eq. 8-89 between $r = R_1$ and $r = R_2$, we obtain:

$$\int_{T_1}^{T_2} k_2 dT = -\frac{q_2'''}{4}(R_2^2 - R_1^2) + \frac{R_2^2}{2}(q_2''' - q_3''') \ell n \left(\frac{R_2}{R_1}\right)$$

which, using Eqs. 8-76 and 8-81, can be written as:

$$\int_{T_2}^{T_1} k_2 dT = \frac{q'_{res}}{4\pi}\left(\frac{\rho_2}{\rho_3}\right)\left[1 - \left(\frac{R_1}{R_2}\right)^2\right]\left(\frac{R_2}{R_{fo}}\right)^2 - \frac{q'_{res}}{4\pi}\left(\frac{\rho_2}{\rho_3}\right)\left(\frac{R_2}{R_{fo}}\right)^2\left(1 - \frac{\rho_3}{\rho_2}\right) \ell n \left(\frac{R_2}{R_1}\right)^2$$

Hence:

$$\int_{T_2}^{T_1} k_2 dT = \frac{q'_{res}}{4\pi}\left(\frac{\rho_2}{\rho_3}\right)\left(\frac{R_2}{R_{fo}}\right)^2\left[1 - \left(\frac{R_1}{R_2}\right)^2 - \left(\frac{\rho_2 - \rho_3}{\rho_2}\right) \ell n \left(\frac{R_2}{R_1}\right)^2\right] \tag{8-92a}$$

Using the notation of Eq. 8-68, Eq. 8-92a can be recast in the form:

$$\int_{T_2}^{T_1} k_2 dT = \frac{q'_{res}}{4\pi}\left(\frac{\rho_2}{\rho_3}\right)\left(\frac{R_2^2 - R_1^2}{R_{fo}^2}\right) F_v\left[\frac{R_2}{R_1}, \frac{R_1}{R_2}\left(\frac{\rho_2}{\rho_2 - \rho_3}\right)^{1/2}\right] \tag{8-92b}$$

E Heat Conduction in Zone 1

Again the integration of the heat conduction equation once leads to:

$$k_1 \frac{dT}{dr} = -q_1''' \frac{r}{2} + \frac{C_1}{r} \tag{8-93}$$

To obtain the value of C_1, we can either use the zero heat flux condition at R_v or the continuity of heat flux at R_1. Applying the boundary condition:

$$\left. k_1 \frac{dT}{dr}\right|_{R_v} = 0 \tag{8-94}$$

leads to

$$C_1 = q'''_1 \frac{R_v^2}{2} \tag{8-95}$$

By integrating Eq. 8-93 again, we get:

$$\int_{T_v}^{T_1} k_1 dT = \frac{-q'''_1}{4}(R_1^2 - R_v^2) + C_1 \ell n \left(\frac{R_1}{R_v}\right) \tag{8-96}$$

Substituting from Eqs. 8-77 and 8-81 for q'''_1 and q'''_3 and Eq. 8-95 for C_1 we get:

$$\int_{T_1}^{T_v} k_1 dT = \frac{q'_{res}}{4\pi}\left(\frac{\rho_1}{\rho_3}\right)\left(\frac{R_1}{R_{fo}}\right)^2 \left[1 - \left(\frac{R_v}{R_1}\right)^2 - \left(\frac{R_v}{R_1}\right)^2 \ell n \left(\frac{R_1}{R_v}\right)^2\right] \tag{8-97a}$$

Using the notation of Eq. 8-68, the last equation can be written as:

$$\begin{aligned}\int_{T_1}^{T_v} k_1 dT &= \frac{q'_{res}}{4\pi}\left(\frac{\rho_1}{\rho_3}\right)\frac{R_1^2 - R_v^2}{R_{fo}^2}\left[1 - \frac{\ell n(R_1/R_v)^2}{\left(\frac{R_1}{R_v}\right)^2 - 1}\right] \\ &= \frac{q'_{res}}{4\pi}\left(\frac{\rho_1}{\rho_3}\right)\left(\frac{R_1^2 - R_v^2}{R_{fo}^2}\right) F_v\left(\frac{R_1}{R_v}, 1\right)\end{aligned} \tag{8-97b}$$

F Solution of the Pellet Problem

Equations 8-75, 8-88, 8-92a (or 8-92b), and 8-97a (or 8-97b) provide a set of four equations in R_1, R_2, R_v, T_{fo}, T_v, and q'. Thus if any two are specified, the rest can be evaluated. Note that the values of T_1 and T_2 are assumed known from Table 8-5.

Generally, two conditions are of interest.

1. A linear heat rate (q'_{res}) and the outer surface temperature (T_{fo}) are specified; so that T_v, along with R_v, R_1, and R_2 can be evaluated.
2. The maximum temperatures (T_v and T_{fo}) are specified; q'_{res} along with R_v, R_1, and R_2 are to be evaluated.

G Two-Zone Sintering

For two-zone representation of the fuel, $R_1 = R_2 = R_s$, $\rho_1 = \rho_2 = \rho_s$, and $T_1 = T_2 = T_s$; Eq. 8-75 reduces to:

$$R_v^2 = \frac{\rho_s - \rho_3}{\rho_s} R_s^2 \tag{8-98}$$

Equation 8-88 takes the form:

$$\int_{T_{fo}}^{T_s} k_3 dT = \frac{q'_{res}}{4\pi}\left[1 - \left(\frac{R_s}{R_{fo}}\right)^2\right] \tag{8-99}$$

Equation 8-92a is not needed. Equation 8-97a takes the form:

$$\int_{T_s}^{T_v} k_s dT = \frac{q'_{res}}{4\pi}\left(\frac{\rho_s}{\rho_3}\right)\left(\frac{R_s}{R_{fo}}\right)^2\left\{1 - \left(\frac{R_v}{R_s}\right)^2\left[1 + \ell n\left(\frac{R_s}{R_v}\right)^2\right]\right\} \quad (8\text{-}100)$$

Example 8-3 Linear power of a two-zone pellet under temperature constraint

PROBLEM Consider an initially solid LMFBR fuel pellet under fixed maximum temperature constraint. Evaluate the linear power (q'_{res}) for the sintered pellet for the same temperature constraint. The sintered pellet may be represented by two zones. Given:

Solid pellet:

$$q' = 14.4 \text{ kW/ft} = 472.8 \text{ W/cm}$$
$$\rho_0 = 88\%\ \rho_{TD}$$
$$T_{fo} = 960°C$$

Two-zone sintered pellet:

$$\rho_s = 98\%\ \rho_{TD}$$
$$T_s = 1800°C$$
$$T_{fo} = 960°C$$

SOLUTION

1. Evaluate the maximum temperature of the solid pellet using Eq. 8-62 for $k = k_{0.88}$:

$$\int_{T_{fo}}^{T_{max}} k_{0.88}\, dT = \frac{q'}{4\pi} = \frac{14.4}{4\pi} = 1.15 \text{ kW/ft} = 37.6 \text{ W/cm}$$

Expressing the conductivity integral in the form represented in Figure 8-2:

$$\int_{100°C}^{T_{max}} k_{0.88}\, dT - \int_{100°C}^{T_{fo}=960°C} k_{0.88}\, dT = 37.6 \text{ W/cm}$$

which yields T_{max} as follows:

$$\int_{100°C}^{T_{max}} k_{0.88}\, dT = 37.6 + 19 = 56.6 \text{ W/cm} \rightarrow T_{max} = 2600°C$$

2. Obtain the relation between q'_{res} and R_s for the restructured pellet. Using Eq. 8-99 for $k_3 = k_{0.88}$, we get:

$$\int_{T_{fo}=960°C}^{T_s=1800°C} k_{0.88}\, dT = \frac{q'_{res}}{4\pi}\left[1 - \left(\frac{R_s}{R_{fo}}\right)^2\right]$$

or

$$17 \text{ W/cm} = \frac{q'_{res}}{4\pi}\left[1 - \left(\frac{R_s}{R_{fo}}\right)^2\right] \quad (8\text{-}101)$$

3. Obtain the relation between q'_{res}, R_{fo}, R_s, and R_v from Eq. 8-100 for $k_s = k_{0.98}$:

$$\int_{T_s = 1800°C}^{T_{max} = 2600°C} k_{0.98} dT = \frac{q'_{res}}{4\pi} \left(\frac{\rho_s}{\rho_0}\right) \left(\frac{R_s}{R_{fo}}\right)^2 \left\{1 - \left(\frac{R_v}{R_s}\right)^2 \left[1 + \ell n \left(\frac{R_s}{R_v}\right)^2\right]\right\}$$

Hence:

$$23.3 = \frac{q'_{res}}{4\pi} \frac{0.98}{0.88} \left(\frac{R_s}{R_{fo}}\right)^2 \left\{1 - \left(\frac{R_v}{R_s}\right)^2 \left[1 + \ell n \left(\frac{R_s}{R_v}\right)^2\right]\right\} \tag{8-102}$$

4. Eliminate q'_{res} between Eqs. 8-101 and 8-102 and rearrange to obtain:

$$0.8125 \left\{1 - \left(\frac{R_v}{R_s}\right)^2 \left[1 + \ell n \left(\frac{R_s}{R_v}\right)^2\right]\right\} = \left(\frac{R_{fo}}{R_s}\right)^2 - 1 \tag{8-103}$$

5. From the mass balance equation (Eq. 8-98) in the solid and sintered pellets:

$$R_v^2 = \frac{\rho_s - \rho_o}{\rho_s} R_s^2 = \frac{0.98 - 0.88}{0.98} R_s^2 = 0.102 R_s^2 \tag{8-98}$$

Thus

$$\left(\frac{R_s}{R_v}\right)^2 = 9.8 \tag{8-104}$$

6. Substituting the value of $(R_v/R_s)^2$ from Eq. 8-104 into Eq. 8-103:

$$0.8125 \{1 - 0.102[1 + \ell n(9.8)]\} = \left(\frac{R_{fo}}{R_s}\right)^2 - 1$$

or

$$R_s/R_{fo} = 0.806 \tag{8-105}$$

7. Substituting the value of R_s/R_{fo} from Eq. 8-105 into Eq. 8-101, we get:

$$q'_{res} = \frac{4\pi(17)}{1 - (0.806)^2} = 609 \text{ W/cm} = 18.57 \text{ kW/ft}$$

i.e., $q'_{res} > q'$. Hence under the same temperature limits, the linear power of a sintered pellet is higher than that of a solid pellet.

Example 8-4 Comparison between three-zone and two-zone fuel pellet maximum temperature

PROBLEM Consider an LMFBR fuel pin operating at a fixed linear power q' of 14.4 kW/ft. Obtain the maximum fuel temperature if the fuel pin is in one of the following restructured conditions.

Three-zone condition
Columnar: $\rho_1 = 98\%\ \rho_{TD}$, $T_1 = 1800°C$
Equiaxed: $\rho_2 = 95\%\ \rho_{TD}$, $T_2 = 1600°C$
Unrestructured: $\rho_3 = 88\%\ \rho_{TD}$, $T_{fo} = 1000°C$

Two-zone condition
Sintered: $\rho_s = 98\%\ \rho_{TD}$, $T_s = 1700°C$
Unrestructured: $\rho_{fo} = 88\%\ \rho_{TD}$, $T_{fo} = 1000°C$

SOLUTION
We note that $q'_{res} = q' = 14.4$ kW/ft $= 472.8$ W/cm.

Case 1

1. We first obtain the value of (R_2/R_{fo}) from Eq. 8-88:

$$\int_{T_{fo}}^{T_2} k_3 dT = \frac{q'}{4\pi}\left[1 - \left(\frac{R_2}{R_{fo}}\right)^2\right] \tag{8-88}$$

where $k_3 = k_{0.88\ TD}$
From Figure 8-2 we get:

$$\int_{1000°C}^{1600°C} k_{0.88}\, dT = 32 - 20 = 12 \text{ W/cm}$$

Hence:

$$\left(\frac{R_2}{R_{fo}}\right)^2 = 1 - \frac{4\pi}{q'}12 = 1 - \frac{48\pi}{472.8} = 1 - 0.32 = 0.68$$

Therefore $R_2 = 0.825\ R_{fo}$

2. Obtain a value for R_1/R_2 from the equation:

$$\int_{T_2}^{T_1} k_2\, dT = \frac{q'}{4\pi}\left(\frac{\rho_2}{\rho_3}\right)\left(\frac{R_2}{R_{fo}}\right)^2\left[1 - \left(\frac{R_1}{R_2}\right)^2 - \left(1 - \frac{\rho_3}{\rho_2}\right)\ell n\left(\frac{R_2}{R_1}\right)^2\right] \tag{8-92a}$$

where $k_2 = k_{0.95\ TD}$.
From Figure 8-2:

$$\int_{1600°C}^{1800°C} k_{0.95}\, dT = 40.2 - 35.7 = 4.5 \text{ W/cm}$$

Substituting in Eq. 8-92a:

$$4.5 = \frac{472.8}{4\pi}\left(\frac{0.95}{0.88}\right)(0.681)\left[1 - \left(\frac{R_1}{R_2}\right)^2 - \left(1 - \frac{0.88}{0.95}\right)\ell n\left(\frac{R_2}{R_1}\right)^2\right]$$

$$4.5 = 27.66\left[1 - \left(\frac{R_1}{R_2}\right)^2 - 0.074\ \ell n\left(\frac{R_2}{R_1}\right)^2\right]$$

$$0.837 = \left(\frac{R_1}{R_2}\right)^2 + 0.074\ \ell n\left(\frac{R_2}{R_1}\right)^2$$

Solving iteratively, we get:

$$\left(\frac{R_1}{R_2}\right)^2 = 0.8226; \text{ and } \left(\frac{R_1}{R_{fo}}\right)^2 = \left(\frac{R_1}{R_2}\right)^2 \left(\frac{R_2}{R_{fo}}\right)^2 = (0.8226)(0.681) = 0.560$$

or $R_1 = 0.907\ R_2$ and $R_1 = 0.748\ R_{fo}$.

3. Determine R_v from the mass balance equation:

$$R_v^2 = \left(\frac{\rho_1 - \rho_2}{\rho_1}\right) R_1^2 + \left(\frac{\rho_2 - \rho_3}{\rho_1}\right) R_2^2 \tag{8-75}$$

or

$$\left(\frac{R_v}{R_2}\right)^2 = \frac{0.98 - 0.95}{0.98}(0.8226) + \frac{0.95 - 0.88}{0.98}$$

$$= 0.02518 + 0.07143 = 0.09661$$

or

$$R_v = 0.311\,R_2 = 0.343 R_1 = 0.256 R_{fo}$$

4. Determine T_v from the integral of the heat conduction equation over zone 1 (Eq. 8-97a):

$$\int_{T_1}^{T_v} k_1\, dT = \frac{q'}{4\pi}\left(\frac{\rho_1}{\rho_3}\right)\left(\frac{R_1}{R_{fo}}\right)^2 \left[1 - \left(\frac{R_v}{R_1}\right)^2 - \left(\frac{R_v}{R_1}\right)^2 \ell n \left(\frac{R_1}{R_v}\right)^2\right]$$

$$= \frac{472.8}{4\pi}\left(\frac{0.98}{0.88}\right)(0.56)$$

$$\left[1 - (0.343)^2 - (0.343)^2\, \ell n \left(\frac{1}{0.343}\right)^2\right]$$

$$= 23.44\ [1 - 0.1176 - 0.2518]$$

$$= 14.78 \text{ W/cm}$$

Because $k_1 = k_{0.98}$, we now have:

$$\int_{1800}^{T_v} k_{0.98}\, dT = 14.78 \text{ W/cm}$$

or, using Figure 8-2:

$$\int_{100°C}^{T_v} k_{0.98}\, dT = 14.78 + \int_{100°C}^{T_1 = 1800°C} k_{0.98}\, dT = 14.78 + 42.5$$

$$= 57.28 \text{ W/cm} \rightarrow T_v = 2340°C$$

Case 2

Consider the two-zone sintered fuel, under the condition $q'_{res} = q'$, and $k_3 = k_{0.88}$.

1. Obtain R_s from the integral of the heat conduction equation over the unrestructured zone (Eq. 8-99):

$$\int_{T_{fo}=1000°C}^{T_s=1700°C} k_{0.88}dT = \frac{q'}{4\pi}\left[1 - \left(\frac{R_s}{R_{fo}}\right)^2\right] = 13.8 \text{ W/cm}$$

Hence:

$$\left(\frac{R_s}{R_{fo}}\right)^2 = 1 - \frac{4\pi}{472.8}(13.8) = 1 - 0.367 = 0.633$$
$$\therefore R_s = 0.796\, R_{fo}$$

2. Obtain R_v from the mass balance equation (Eq. 8-98):

$$R_v^2 = \left(\frac{\rho_s - \rho_o}{\rho_s}\right) R_s^2 = \frac{0.98 - 0.88}{0.98} R_s^2$$

i.e.,

$$R_v^2 = 0.102\, R_s^2$$
$$R_v = 0.319\, R_s = 0.2543\, R_{fo}$$

3. Obtain T_v from the heat conduction integral (Eq. 8-100) when $k_s = k_{0.98}$:

$$\int_{1700°C}^{T_v} k_s\, dT = \frac{q'}{4\pi}\left(\frac{\rho_s}{\rho_o}\right)\left(\frac{R_s}{R_{fo}}\right)^2\left[1 - \left(\frac{R_v}{R_s}\right)^2 - \left(\frac{R_v}{R_s}\right)^2 \ell n \left(\frac{R_s}{R_v}\right)^2\right] \quad (8\text{-}100)$$

or

$$\int_{100°C}^{T_v} k_{0.98}\, dT = \int_{100°C}^{1700°C} k_{0.98}\, dT + \frac{472.8}{4\pi}\left(\frac{0.98}{0.88}\right)(0.633)$$
$$\left[1 - 0.102 - 0.102\, \ell n \left(\frac{1}{0.102}\right)\right]$$
$$= 40 + 26.50\,(1 - 0.102 - 0.232)$$
$$= 40 + 26.50\,(0.666)$$
$$= 57.65 \text{ w/cm}$$
$$\rightarrow T_v = 2360°C$$

Although the three region model is a more exact one, there is only a small advantage in using the three-zone approach, in that T_v from the three-zone model is 20°C lower than that from the two-zone approach.

H Comments on Design Implications of Restructured Fuel

The result of fuel sintering is to reduce the effective thermal resistance between the highest fuel temperature (T_{max}) and the pellet outer temperature (T_{fo}). Thus two operational options exist after restructuring.

1. If the fuel maximum temperature is kept constant, the linear power can be increased. This condition is applicable to the LMFBRs, as the heat flux to the

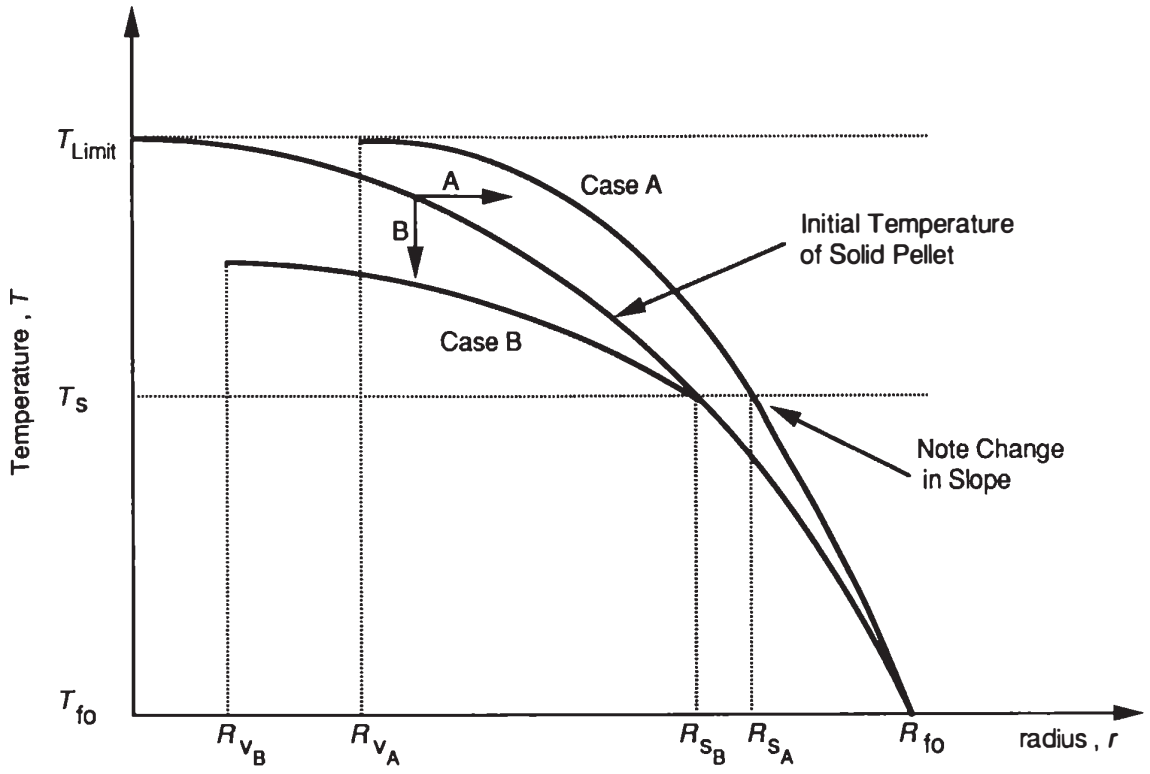

Case A	$T_{max,A} = T_{max,initial} = T_{limit}$
Case B	$q'_{initial} = q'_B$

Figure 8-16 Design and irradiation strategies for initially solid fuel pellets.

coolant is not a limiting factor. This case is depicted graphically as case A in Figure 8-16. The assumption of a constant T_{fo} in the figure implies that the coolant conditions have been adjusted.

2. If the linear power is kept constant, the fuel maximum temperature is reduced. This case may be applicable to LWRs, as other considerations limit the operating heat flux of a fuel pin. This case is depicted graphically as case B in Figure 8-16. If the fuel maximum temperature is calculated ignoring the sintering process, a conservative value is obtained.

VII THERMAL RESISTANCE BETWEEN FUEL AND COOLANT

The overall thermal resistance between the fuel and coolant consists of (1) the resistance of the fuel itself, (2) the resistance of the gap between the fuel and the cladding, (3) the resistance of the cladding, (4) the resistance of the coolant.

For typical LWR and LMFBR fuel rods, the resistance of the UO_2 fuel is by far the largest, as can be inferred from the temperature profile of Figure 8-17. The next

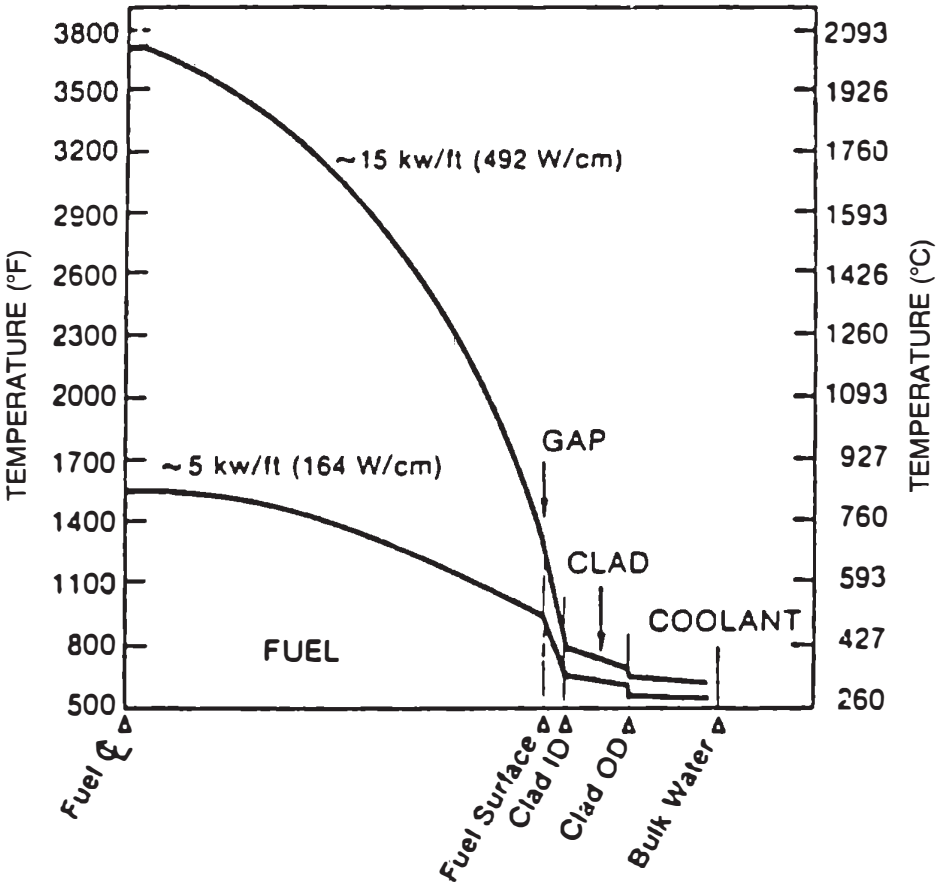

Figure 8-17 Typical PWR fuel rod temperature profile for two LHGRs. *(From Jordan [12].)*

largest resistance is that of the gap. Hence models for the gap conductance with increasing sophistication have been developed over the years. In this section, the gap resistance models are presented first, and then the overall resistance is discussed.

A Gap Conductance Models

It is usually assumed that the gap consists of an annular space occupied by gases. The gas composition is initially the fill gas, which should be an inert gas such as helium, but is gradually altered with burnup by the addition of gaseous fission product such as xenon and krypton. (Sodium-cooled reactors have also considered sodium bonding.) However, this simple picture does not reflect the real conditions of the fuel pin after some irradiation. The fuel pellets usually crack upon irradiation, as shown in Figure 8-18, and this situation leads to circumferential variation in the gap. In addition, thermal expansions of the fuel and cladding are often different, the result being substantial pellet–cladding contact at the interface. This contact reduces the thermal resistance and hence effectively increases the "gap" conductance of the burnup. It occurs despite the lower conductivity of the fission gas products, compared to the initial conductivity of helium. A typical change of gap conductance with burnup is shown in Figure 8-19.

Figure 8-18 Example of a cracked fuel cross section. *(From Clark et al. [4].)*

1 As-fabricated gap. The gap conductance at the as-fabricated condition of tne fuel can be modeled as due to conduction through an annular space as well as to radiation from the fuel. Thus the heat flux at an intermediate gap position can be given by:

$$q''_g = h_g(T_{fo} - T_{ci}) \tag{8-106}$$

where for an open gap:

$$h_{g,open} = \frac{k_{gas}}{\delta_{eff}} + \frac{\sigma}{\dfrac{1}{\epsilon_f} + \dfrac{1}{\epsilon_c} - 1} \frac{T_{fo}^4 - T_{ci}^4}{T_{fo} - T_{ci}} \tag{8-107a}$$

where $h_{g,open}$ = heat transfer coefficient for an open gap; T_{fo} = fuel surface temperature; T_{ci} = clad inner surface temperature; k_{gas} = thermal conductivity of the gas; δ_{eff} = effective gap width; σ = Stefan-Boltzman constant; ϵ_f, ϵ_c = surface emissivities of the fuel and cladding, respectively.

Equation 8-107a can often be approximated by:

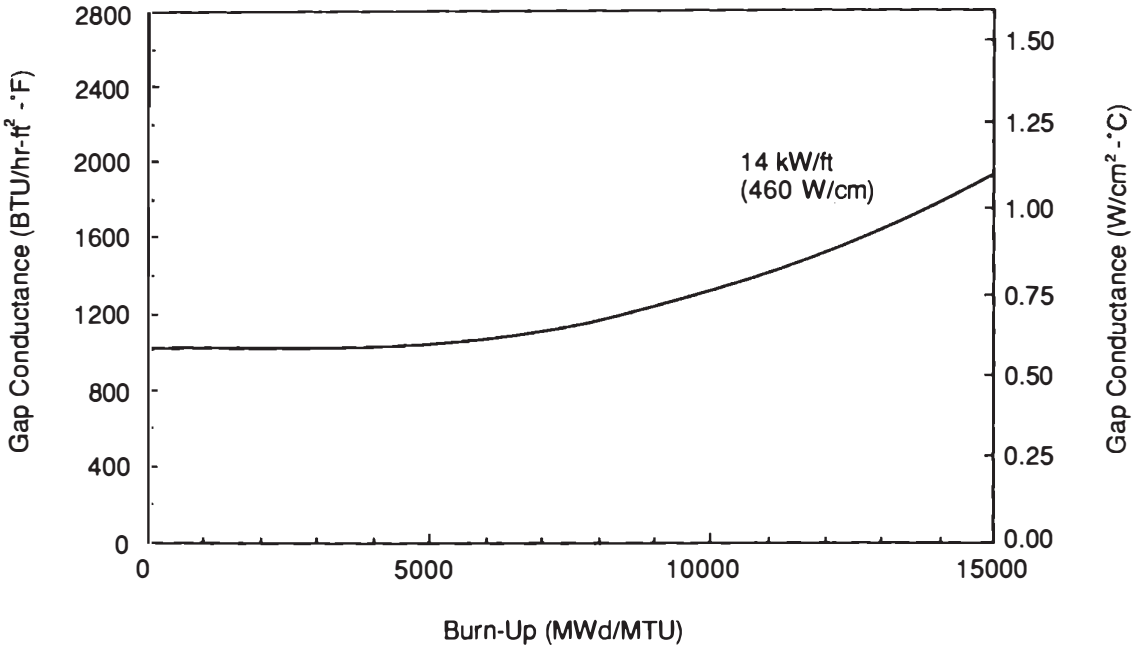

Figure 8-19 Variations of gap conductance with burnup for a PWR fuel rod (pressurized with helium) and operating at 14 kW/ft (460 W/cm). *(From Fenech [6].)*

$$h_{g,open} = \frac{k_{gas}}{\delta_{eff}} + \frac{\sigma T_{fo}^3}{\frac{1}{\epsilon_f} + \frac{1}{\epsilon_c} - 1} \tag{8-107b}$$

It should be noted that the effective gap width is larger than the real gap width because of the temperature discontinuities at the gas–solid surface. The temperature discontinuities arise near the surface owing to the small number of gas molecules present near the surface. Thus it is possible to relate δ_{eff} to the real gap width (δ_g), as illustrated in Figure 8-20, by:

$$\delta_{eff} = \delta_g + \delta_{jump1} + \delta_{jump2} \tag{8-108}$$

At atmospheric pressure, $\delta_{jump1} + \delta_{jump2}$ were found to equal 10 μm in helium and 1 μm in xenon [23].

The gas conductivity of a mixture of two gases is given by [13]:

$$k_{gas} = (k_1)^{x_1} (k_2)^{x_2} \tag{8-109}$$

where x_1 and x_2 are the mole fractions of gases 1 and 2, respectively. For rare gases the conductivity dependence on temperature is given by [26]:

$$k(\text{pure gas}) = A \times 10^{-6} T^{0.79} \text{ W/cm °K} \tag{8-110}$$

where T is in °K and A = 15.8 for helium, 1.97 for argon, 1.15 for krypton, and 0.72 for xenon.

2 Gap closure effects. Calza-Bini et al. [3] observed that the model of Eqs. 8-106 to 8-108 provides a reasonable estimate for the gap conductance on the first rise to power. Subsequently, the measured gap conductance increased and was attributed to

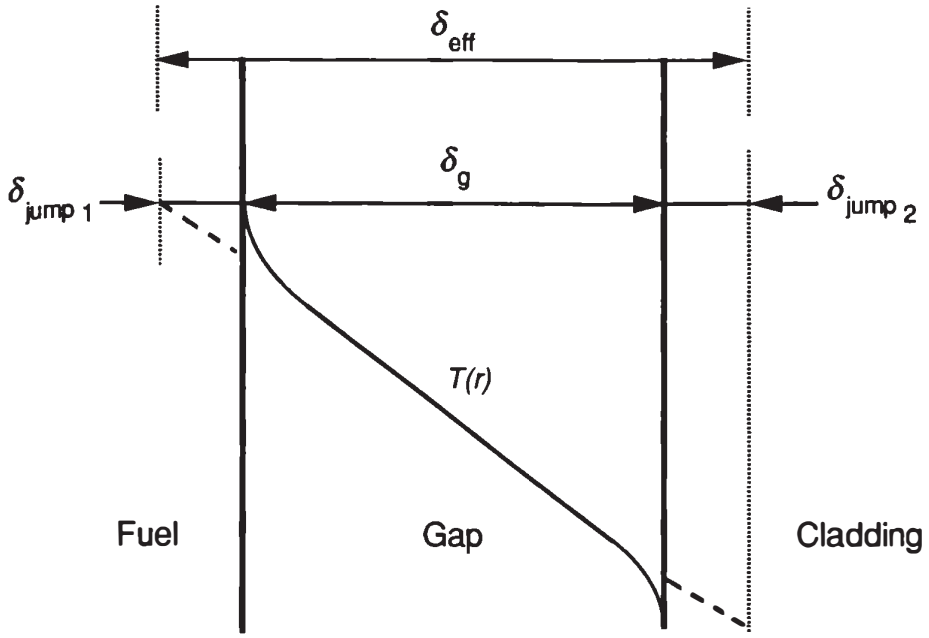

Figure 8-20 Temperature profile across the fuel–clad gap.

a portion of the fuel contacting the cladding and, after fuel cracking, remaining in contact. Additionally, cracking has a negative effect on thermal conductivity of the fuel (see section III.A.5).

When gap closure occurs because of fuel swelling and thermal expansion, the contact area with the cladding is proportional to the surface contact pressure between the fuel and cladding (Fig. 8-21). Thus the contact-related heat transfer coefficient can be given by:

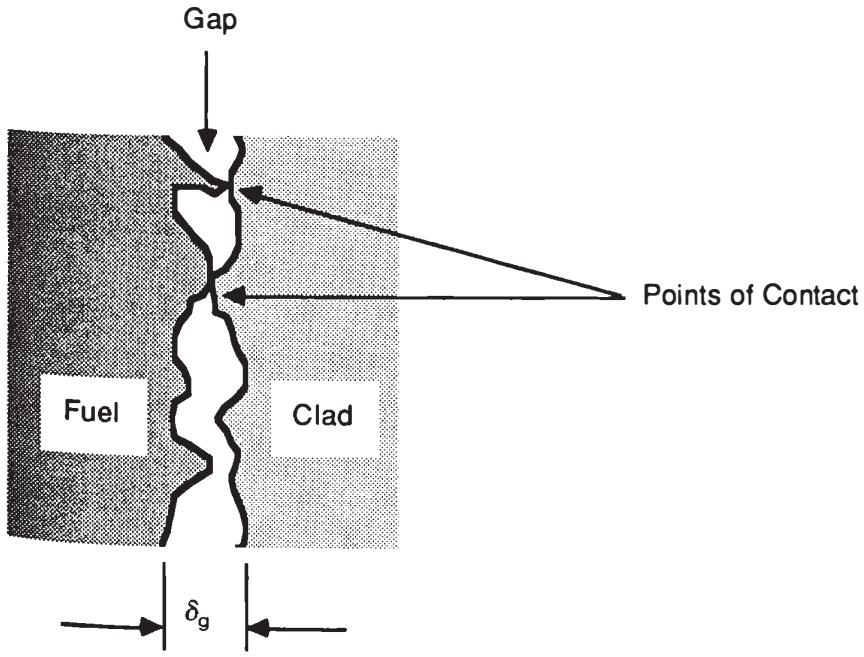

Figure 8-21 Close-up view of fuel--clad contact.

$$h_{contact} = C \frac{2k_f k_c}{k_f + k_c} \frac{p_i}{H\sqrt{\delta_g}} \text{ (Btu/ft}^2 \text{ hr)} \tag{8-111}$$

where C = a constant ($= 10\ \text{ft}^{-1/2}$); p_i = surface contact pressure (psi) (usually calculated based on the relative thermal expansion of the fuel and the cladding, but ignoring the elastic deformation of the cladding); H = Meyer's hardness number of the softer material (typical values are, for steel, 13×10^4 psi and, for zircaloy, 14×10^4 psi); δ_g = mean thickness of the gas space (feet) (calculated based on the roughness of the materials in contact); k_f and k_c = thermal conductivities of fuel and cladding (Btu/hr ft °F).

The total gap conductance upon contact may be given by:

$$h_g = h_{g,open} + h_{contact} \tag{8-112}$$

Ross and Stoute [23] have shown that the general features of Eqs. 8-111 and 8-112 can be observed in experiments. From their data they concluded that δ_{jump} is 1 to 10 μm at atmospheric pressure, which is 10 to 30 times the gas molecule mean free path. Jacobs and Todreas [11] used the work of Cooper et al. [5] to formulate a better model by recognizing the nonuniform distribution of the surface protrusions. Yet even their improved model could not explain all the experimental observations. Thus inadequacies in modeling remain to be resolved. The effect of increased swelling at higher linear powers is to increase the gap conductance unless the initial gap thickness is so small as to lead to saturation of the contact effect, as can be observed in Figure 8-22. The reader should consult the empirically based relations available in the database of MATPRO for additional information [21].

B Overall Resistance

The linear power of a cylindrical fuel pin can be related to the temperature drop ($T_{max} - \bar{T}_m$) by considering the series of thermal resistances posed by the fuel, the gap, the cladding, and the coolant. Consider, for simplicity, a solid fuel pellet with a constant thermal conductivity ($\bar{k}_f$). From Eq. 8-62, we get:

$$T_{max} - T_{fo} = \frac{q'}{4\pi\bar{k}_f} \tag{8-113}$$

Across the gap the temperature drop is predicted from Eq. 8-106 by:

$$T_{fo} - T_{ci} = \frac{q''_g}{h_g} = \frac{2\pi R_g q''_g}{2\pi R_g h_g} = \frac{q'}{2\pi R_g h_g} \tag{8-114}$$

where R_g = mean radius in the gap; h_g = effective gap conductance.

For a thin cladding a linear temperature drop across the cladding may be assumed. Hence the temperature drop across the cladding is given by:

$$T_{ci} - T_{co} = \frac{q''}{k_c/\delta_c} = \frac{q'}{2\pi R_c k_c/\delta_c} \tag{8-115a}$$

where R_c = mean radius in the cladding.

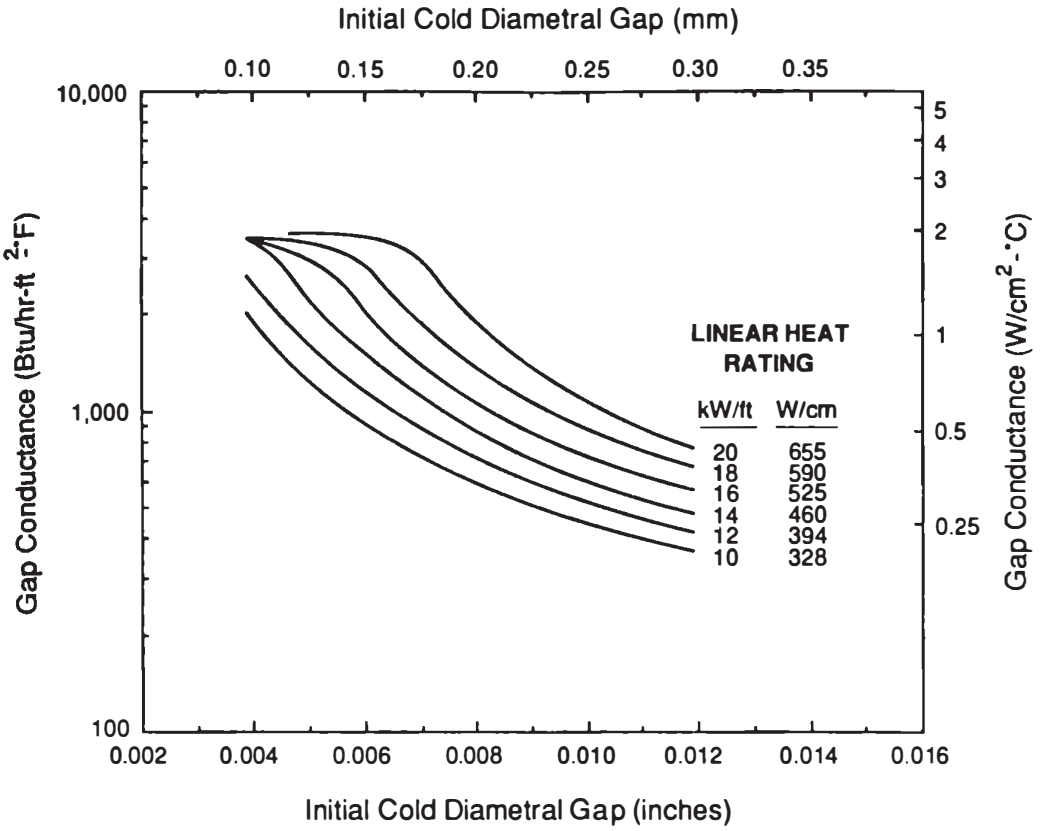

Figure 8-22 Calculated gap conductance as a function of cold diametral gap in a typical LWR fuel rod. *(From Horn and Panisko, [10].)*

The temperature drop across a thick clad can be determined as:

$$T_{ci} - T_{co} = \frac{q'}{2\pi k_c} \ell n \left(\frac{R_{co}}{R_{ci}}\right) \tag{8-115b}$$

The heat flux emerging from the cladding is given by

$$q''_{co} = h(T_{co} - T_m) \tag{8-116}$$

where T_m = mean coolant temperature at the cross section. The heat transfer coefficient (h) is dependent on the coolant flow conditions. The linear power is then given by:

$$q' = 2\pi R_{co} q''_{co} = 2\pi R_{co} h(T_{co} - T_m) \tag{8-117}$$

Equation 8-117 can be recast to give the temperature drop $(T_{co} - T_m)$:

$$T_{co} - T_m = \frac{q'}{2\pi R_{co} h} \tag{8-118}$$

Hence the linear power of the pin can be related to an overall thermal resistance and the temperature drop $T_{max} - T_m$ (from Eqs. 8-113, 8-114, 8-115b, and 8-118):

$$T_{max} - T_m = q' \left[\frac{1}{4\pi \bar{k}_f} + \frac{1}{2\pi R_g h_g} + \frac{1}{2\pi k_c} \ell n \left(\frac{R_{co}}{R_{ci}}\right) + \frac{1}{2\pi R_{co} h}\right] \tag{8-119}$$

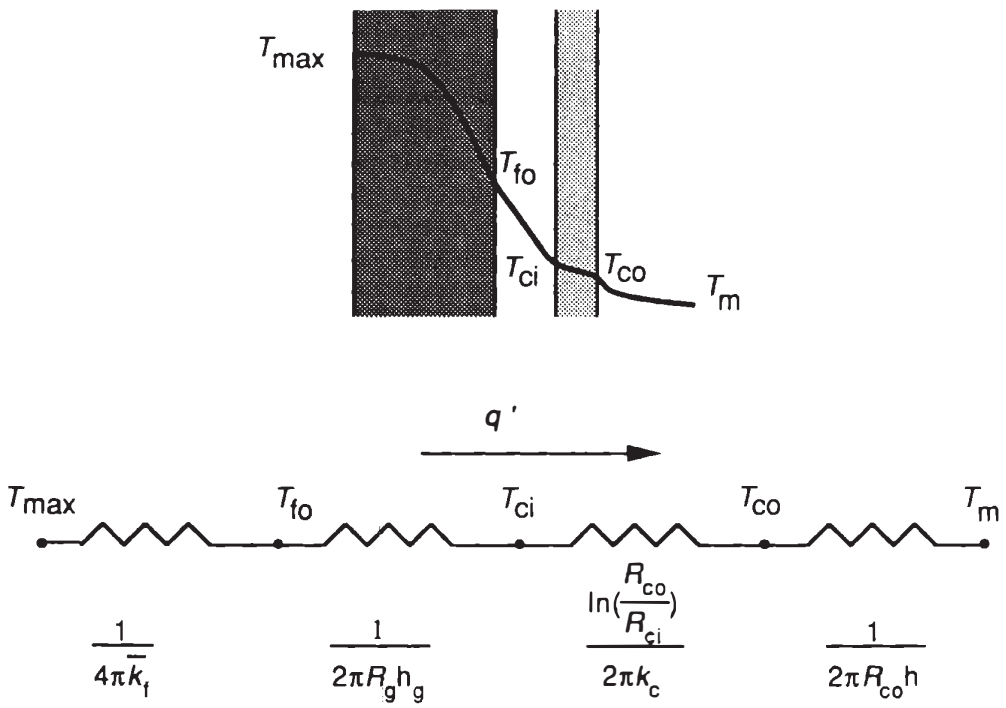

Figure 8-23 Thermal resistance analogy circuit for a cylindrical fuel pin.

The linear power is then analogous to an electrical current driven by the potential $T_{max} - T_m$ across a series of resistances, as depicted in Figure 8-23. This concept can be used to analyze the rate of temperature change in the fuel during a transient, provided the transient is sufficiently slow to allow the quasi-steady-state treatment of the thermal resistance.

REFERENCES

1. Arpaci, V. S. *Conduction Heat Transfer*. Menlo Park, CA: Addison-Wesley, 1966.
2. Biancharia, A. The effect of porosity on thermal conductivity of ceramic bodies. *Trans. ANS* 9:15, 1966.
3. Calza-Bini, A., et al. In-pile measurement of fuel cladding conductance for pelleted and vipac zircaloy-2 sheathed fuel pin. *Nucl. Technol.* 25:103, 1975.
4. Clark, P. A. E., et al. *Post Irradiation Examination of Two High Burnup Fuel Rods Irradiated in the Halden BWR*. AEREG3207, AERE Harwell Report. May 1985.
5. Cooper, M. G., Mikic, B. B., and Yovanovich, M. M. Thermal contact conductance. *Int. J. Heat Mass Transfer* 12:279, 1969.
6. Fenech, H. General considerations on thermal design and performance requirements of nuclear reactor cores. In H. Fenech (ed.), *Heat Transfer and Fluid Flow in Nuclear Systems*. Oxford: Pergamon Press, 1981.
7. Francl, J., and Kingery, W. D. Thermal conductivity. IX. Experimental investigation of effect of porosity on thermal conductivity. *J. Am. Ceram. Soc.* 37:99, 1954.
8. Gibby, R. L. The effect of plutonium content on the thermal conductivity of (U, Pu)O_2 solid solutions. *J. Nucl. Mater.* 38:163, 1971.
9. Hann, C. R., et al. *GAPCON-Thermal-7: A Computer Program for Calculating the Gap Conductance in Oxide Fuel Pins*. BNWL-1778, September 1973.
10. Horn, G. R., and Panisko, F. E. HEDL-TME72-128, September 1979.

11. Jacobs, G., and Todreas, N. Thermal contact conductance in reactor fuel elements. *Nucl. Sci. Eng.* 50:282, 1973.
12. Jordan, R. MIT Reactor Safety Course, 1979.
13. Kampf, H., and Karsten, G. Effects of different types of void volumes on the radial temperature distribution of fuel pins. *Nucl. Appl. Technol.* 9:288, 1970.
14. Latta, R. E., and Fryxell, R. E. Determination of solidus–liquidus temperatures in the UO_{2+n} system ($-0.50 < n < 0.20$). *J. Nucl. Mater.* 35:195, 1970.
15. Loeb, A. L. Thermal conductivity. VIII. A theory of thermal conductivity of porous material. *J. Am. Ceram. Soc.* 37:96, 1954.
16. MacDonald, P. E., and Smith, R. H. An empirical model of the effects of pellet cracking on the thermal conductivity of UO_2 light water reactor fuel. *Nucl. Eng. Design* 61:163, 1980.
17. MacDonald, P. E., and Weisman, J. Effect of pellet cracking on light water reactor fuel temperatures. *Nucl. Technol.* 31:357, 1976.
18. Marr, W. M., and Thompson, D. H. *Trans. Am. Nucl. Soc.* 14:150, 1971.
19. Notley, M. J. F. A computer model to predict the performance of UO_2 fuel element irradiated at high power output to a burnup of 10,000 MWD/MTU. *Nucl. Appl. Technol.* 9:195, 1970.
20. Olander, D. R. *Fundamental Aspects of Nuclear Reactor Fuel Elements.* T1D-26711-P1, 1976.
21. Olsen, C. S., and Miller, R. L. *MATPRO, Vol. II: A Handbook of Materials Properties for Use in the Analysis of Light Water Reactor Fuel Behavior.* NUREG/CR-0497, USNRC, 1979.
22. Reymann, G. A. *MATPRO* (Vol. II).
23. Ross, A. M., and Stoute, R. L. *Heat Transfer Coefficient between UO_2 and Zircaloy-2.* AECL-1552, 1962.
24. Schmidt, H. E., and Richter, J. Presented at the Symposium on Oxide Fuel Thermal Conductivity, Stockholm, 1967.
25. Todreas, N. E. Pressurized subcooled light water systems. In H. Fenech (ed.), *Heat Transfer and Fluid Flow in Nuclear Systems.* Oxford: Pergamon Press, 1981.
26. Von Ubisch, H., Hall, S., and Srivastov, R. Thermal conductivities of mixtures of fission product gases with helium and argon. Presented at the 2nd U.N. International Conference on Peaceful Uses of Atomic Energy, Sweden, 1958.
27. Zebroski, E. L., Lyon, W. L., and Bailey, W. E. Effect of stoichiometry on the properties of mixed oxide U-Pu fuel. In: *Proceedings of the Conference on Safety, Fuels, and Core Design in Large Fast Power Reactors,* 11–14 October, 1965. USAEC Report ANL-7120, p. 382, Argonne National Laboratory, 1965.

PROBLEMS

Problem 8-1 Application of Kirchoff's law to pellet temperature distribution (section II)

For PWR cylindrical solid fuel pellet operating at a heat flux equal to 1.7 MW/m^2 and a surface temperature of 400°C, calculate the maximum temperature in the pellet for two assumed values of conductivities.

1. k = 3 W/m °C independent of temperature
2. $k = 1 + 3e^{-0.0005T}$ where T is in °C

UO_2 pellet diameter = 10.0 mm
UO_2 density 95% theoretical density
Answers: 1. T_{max} = 1817°C
2. T_{max} = 1974°C

Problem 8-2 Effect of cracking on UO_2 conductivity (section III)

For the conditions given in Example 8-1, evaluate the effective conductivity of the UO_2 pellet after cracking using the empiric relation of Eq. 8-24. Assume the gas is helium at a temperature $T_{gas} = 0.7\ T_{cl} + 0.3\ T_f$. Compare the results to those obtained in Example 8-1.

Answer: k_{eff} = 1.67 W/m°K

Problem 8-3 Comparison of UO_2 and UC fuel temperature fields (section IV)

A fuel plate is of half width a = 10 mm and is clad in a zircaloy sheet of thickness δ_c = 2 mm. The heat is generated uniformly in the fuel.

Compare the temperature drop across the fuel plate when the fuel is UO_2 with that of a UC fuel for the same heat-generation rate (i.e., calculate the ratio of $T_{max} - T_{co}$ for the UC plate to that of the UO_2 plate).

Answer: $\Delta T_{UO_2}/\Delta T_{UC} = 4.15$

Problem 8-4 Temperature fields in fresh and irradiated fuel (section V)

Consider two conditions for heat transfer in the pellet and the pellet–clad gap of a BWR fuel pin.

- Initial uncracked pellet with no relocation
- Cracked and relocated fuel

1. For each combination, find the temperatures at the clad inner surface, the pellet outer surface, and the pellet centerline.
2. Find for each case the volume-weighted average temperature of the pellet.

Geometry and material information
Clad outside diameter = 12.52 mm
Clad thickness = 0.86 mm
Fuel–clad diametral gap = 230 μm
Initial solid pellet with density = 88%

Basis for heat transfer calculations
Clad conductivity is constant at 17 W/m °K
Gap conductance
  Without fuel relocation, 4300 W/m² °K,
  With fuel relocation, 31,000 W/m² °K;
Fuel conductivity (average) at 95% density
  Uncracked, 2.7 W/m °K,
  Cracked, 2.4 W/m °K;
Volumetric heat deposition rate: uniform in the fuel and zero in the clad

Do not adjust the pellet conductivity for restructuring.
Use Biancharia's porosity correction factor (Eq. 8-21).

Operating conditions
Clad outside temperature = 295°C
Linear heat-generation rate = 44 kW/m

Answers:

	Uncracked	*Cracked*
1. T_{max} (°C)	2112	2027
T_{fo} (°C)	664	398
T_{ci} (°C)	355.9	355.9
2. T_{ave} (°C)	1388	1213

Problem 8-5 Temperature field in a restructured fuel pin (section VI)

Using the conditions of Problem 8-4 for the uncracked fuel, calculate the maximum fuel temperature for the given operating conditions. Assume two-zone sintering, with $T_{sintering}$ = 1700°C and $\rho_{sintered}$ = 98% TD.

Answer: T_v = 2140°C

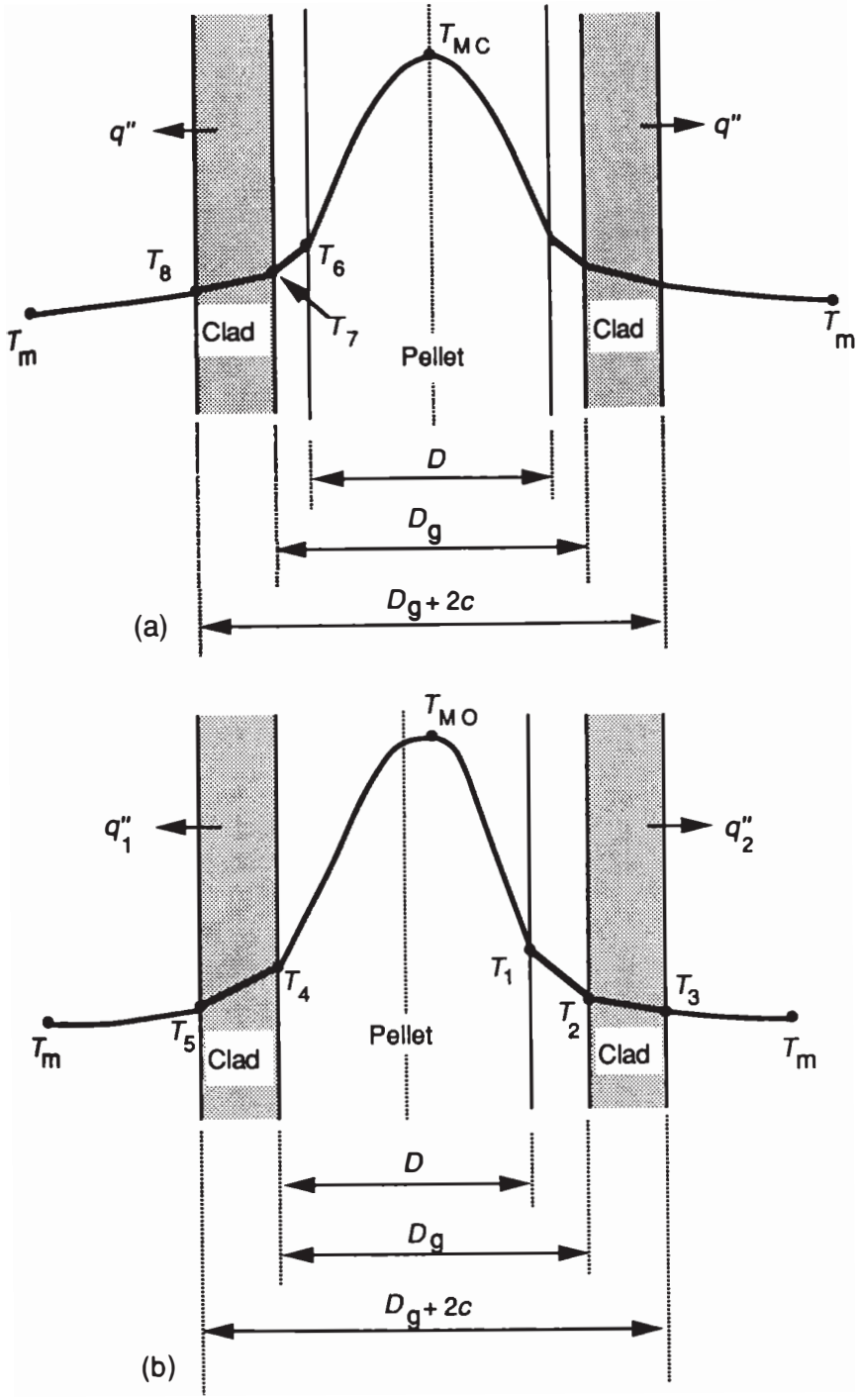

Figure 8-24 Effect of fuel offset. (*a*) Centered fuel pellet. (*b*) Effect of fuel pellet offset.

Problem 8-6 Eccentricity effects in a plate-type fuel (section VII)

A nuclear fuel element is of plate geometry (Fig. 8-24). It is desired to investigate the effects of fuel offset within the clad. For simplicity, assume uniform heat generation in the fuel, temperature-independent fuel conductivity, and heat conduction only in the gap. Calculate:

1. The temperature difference between the offset fuel and the concentric fuel maximum temperatures:

$$T_{MO} - T_{MC}$$

2. The temperature difference between the cladding maximum temperatures:

$$T_7 - T_4$$

3. The ratio of heat fluxes to the coolant.

$$\frac{q''}{q_1''} \quad \text{and} \quad \frac{q''}{q_2''}$$

$T_{coolant}$ and heat transfer coefficient to coolant may be assumed constant on both sides and for both cases. Neglect interface contact resistance for fuel and clad.

$k_f = 3.011$ W/m°C ($PuO_2 - UO_2$)
$k_g = 0.289$ W/m°C (He)
$k_c = 21.63$ W/m°C (SS)
$D = 6.352$ mm
$D_g = 6.428$ mm
$c = 0.4054$ mm
$q''' = 9.313 \times 10^5$ kW/m^3
$h_{coolant} = 113.6$ kW/m^2°C (Na)

Answer: 1. $T_{MO} - T_{MC} = -23.9$°C
2. $T_7 - T_4 = -8.83$°C
3. $\frac{q_1''}{q''} = 1.109$ and $\frac{q_2''}{q''} = 0.8914$

Problem 8-7 Determining the linear power given a constraint on the fuel average temperature (section VII)

For a PWR fuel pin with pellet radius of 4.7 mm, clad inner radius of 4.89 mm, and outer radius of 5.46 mm, calculate the maximum linear power that can be obtained from the pellet such that the mass average temperature in the fuel does not exceed 1204°C (2200°F). Take the bulk fluid temperature to be 307.5°C and the coolant heat transfer coefficient to be 28.4 kW/m^2 °C. In the gap, consider only conduction heat transfer.

Fuel conductivity (k_f) = 3.011 W/m °C
Clad conductivity (k_c) = 18.69 W/m °C
Helium gas conductivity (k_g) = 0.277 W/m °C

Answer: $q' = 22.9$ kW/m

CHAPTER
NINE

SINGLE-PHASE FLUID MECHANICS

I APPROACH TO SIMPLIFIED FLOW ANALYSIS

The objective of the fluid mechanics analysis is to provide the velocity and pressure distributions in a given geometry for specified boundary and initial conditions. The transport equations of mass, momentum, and energy were derived for both a control volume and at a local point in Chapter 4. Theoretically, we need to solve these detailed equations simultaneously to obtain the velocity, pressure, and temperature distributions in the flow system of interest. Practically, however, we first simplify the equations to be solved by eliminating insignificant terms for the situation of interest.

Furthermore, our objective can often be achieved by applying the accumulated engineering experience in a manner that empirically relates macroscopic quantities, e.g., the pressure drop and the flow rate through a tube, without obtaining the detailed distribution of the fluid velocity or density in the tube. This engineering approach can be used whenever the flow characteristics fall within the range of previously established empiric relations.

The analytic approach and the empiric engineering relations for single-phase flow analysis are discussed in this chapter. The heat transport analysis is dealt with in Chapter 10, and the fluid mechanics of two-phase flow are considered in Chapter 11.

A Solution of the Flow Field Problem

Determination of the velocity field in a moving fluid requires simultaneous solution of the mass, momentum, and energy equations:

$$\text{Mass: } \frac{\partial}{\partial t}\rho + \nabla \cdot \rho\vec{v} = 0 \tag{4-73}$$

$$\text{Linear momentum: } \frac{\partial}{\partial t}\rho\vec{v} + \nabla \cdot \rho\vec{v}\vec{v} = \nabla \cdot (\overline{\overline{\tau}} - p\,\overline{\overline{I}}) + \rho\vec{g} \tag{4-80}$$

Energy, in one of its various forms, e.g.,

$$\frac{\partial}{\partial t}\rho u^\circ + \nabla \cdot \rho u^\circ \vec{v} = -\nabla \cdot \vec{q}'' + \nabla \cdot (\overline{\overline{\tau}} - p\,\overline{\overline{I}}) \cdot \vec{v} + q' + \rho\vec{v} \cdot \vec{g} \tag{4-96}$$

or equivalently:

$$\rho c_p \frac{DT}{Dt} = -\nabla \cdot \vec{q}'' + q''' + \beta T \frac{Dp}{Dt} + \Phi \tag{4-122a}$$

There are six unknowns in the above equations: ρ, $\vec{v}$, u° (or T), p, $\overline{\overline{\tau}}$, and $\vec{q}''$. Two additional quantities are a priori given, q''' and $\vec{g}$. Therefore the three transport equations need to be supplemented with three additional equations: the equation of state for the fluid:

$$\rho = \rho(p,T) \tag{5-61}$$

and two constitutive equations that relate shear stress and heat flux to the unknown or given quantities (in magnitude as well as spatial gradients):

$$\overline{\overline{\tau}} = \overline{\overline{\tau}}(\rho,\vec{v},T) \tag{5-62}$$

$$\vec{q}'' = \vec{q}''(\rho,\vec{v},T) \tag{5-63}$$

Note that T in Eqs. 5-61 through 5-63 can be replaced by u° if the energy equations in the form 4-96 is used.

Finally, initial and boundary conditions necessary for completely specifying the solution of the differential transport equations should be supplied.

Thus given q''' and $\vec{g}$, the above six equations can be solved to obtain the six variables ρ, $\vec{v}$, T (or u°), p, $\overline{\overline{\tau}}$, $\vec{q}''$.

Often, however, we tend to use simplified forms that represent acceptable approximations to the physical conditions. Thus the complexity of the problem can be reduced, and even analytic forms for all the variables may be obtained.

B Possible Simplifications

1. The most significant of these approximations is the assumption of temperature-independent physical properties, which leads to decoupling of the velocity field solution from the energy equation, as both ρ and $\overline{\overline{\tau}}$ no longer depend on T. Thus Eqs. 4-73 and 4-80 can then be solved along with the simplified equations:

$$\rho = \rho(p) \tag{5-61}$$

$$\overline{\overline{\tau}} = \overline{\overline{\tau}}(\rho,\vec{v}) \tag{5-62}$$

to obtain the unknowns ρ, $\vec{v}$, p, $\overline{\overline{\tau}}$. This assumption removes the energy equation from the system of equations to be solved, as illustrated in Figure 9-1. This assumption is good in flow fields that do not span a wide range of temperatures, provided the

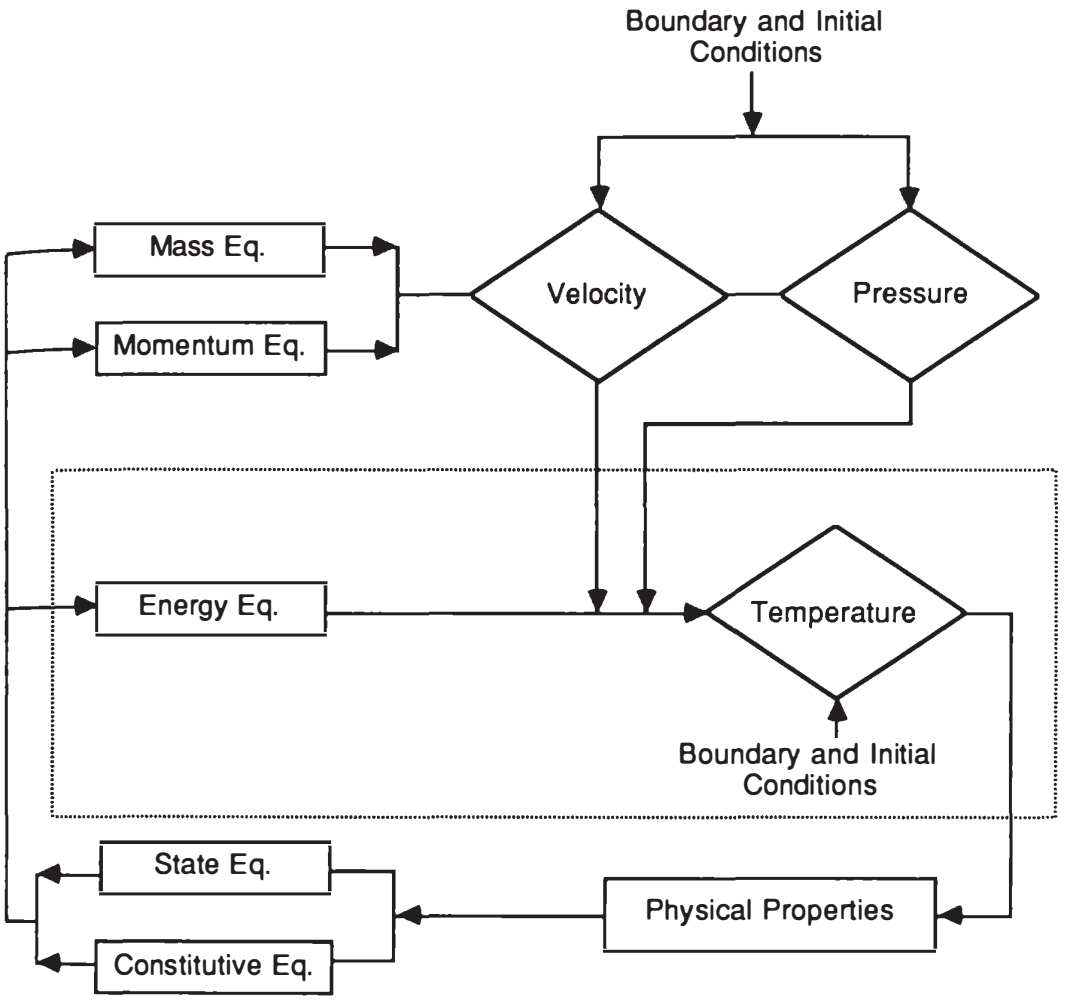

Figure 9-1 Fluid mechanics analysis schemes. The region within the dotted line is considered separately when the physical properties are assumed temperature independent. Note that in a transient situation the initial conditions for each time period (one time step) are the values of the variable at the end of the preceding time period.

selection for $\rho(p)$ and $\overline{\overline{\tau}}(\rho,\vec{v})$ is made to represent their values at an appropriate temperature within the range of interest.

Other possible simplifying assumptions are:

2. The density (ρ) is constant, which is a valid assumption when the effect of pressure as well as temperature is small. This is an incompressible flow problem with constant-temperature properties. It is a reasonable assumption for nearly all practical problems involving liquids. At high pressure it may also be applied to gases if the pressure variation within the system is small.

3. The effects of viscosity are negligible, so that $\nabla \cdot \overline{\overline{\tau}}$ is a negligible term in the momentum equation. This is called an inviscid flow problem and is appropriate for flows where the momentum effects dominate, such as the case at high flow velocities in large compartments or even with open channel flow. In some nuclear reactor components, e.g., large pipes, or within a large reactor vessel plenum, the flow may be considered inviscid.

4. The problem can be solved in the fewest reasonable number of dimensions. For example, a problem can be solved as one-dimensional if the flow in the other